EUROPEAN RESPIRATORY *journal*

FLAGSHIP SCIENTIFIC JOURNAL OF ERS

Early View

Original research article

Activation of immune cell proteasomes in peripheral blood of smokers and COPD patients - implications for therapy

Ilona E. Kammerl, Sophie Hardy, Claudia Flexeder, Andrea Urmann, Julia Peierl, Yuqin Wang, Oliver Vosyka, Marion Frankenberger, Katrin Milger, Jürgen Behr, Andrea Koch, Juliane Merl-Pham, Stefanie M. Hauck, Charles Pilette, Holger Schulz, Silke Meiners

Please cite this article as: Kammerl IE, Hardy S, Flexeder C, *et al.* Activation of immune cell proteasomes in peripheral blood of smokers and COPD patients - implications for therapy. *Eur Respir J* 2021; in press (https://doi.org/10.1183/13993003.01798-2021).

Activation of immune cell proteasomes in peripheral blood of smokers and COPD patients - implications for therapy

Ilona E. Kammerl[1], Sophie Hardy[1,2], Claudia Flexeder[3], Andrea Urmann[1], Julia Peierl[1], Yuqin Wang[1], Oliver Vosyka[1], Marion Frankenberger[1,4], Katrin Milger[1,5], Jürgen Behr[1,5], Andrea Koch[1,6], Juliane Merl-Pham[7], Stefanie M. Hauck[7], Charles Pilette[2], Holger Schulz[3], Silke Meiners[1]

[1] Comprehensive Pneumology Center (CPC), University Hospital, Ludwig-Maximilians-University, Helmholtz Zentrum München, Member of the German Center for Lung Research (DZL), Munich, Germany

[2] Cliniques universitaires Saint-Luc, department of pulmonology, and Institute of Experimental and Clinical Research (IREC), Pole of pulmonology, ENT and dermatology, Université catholique de Louvain, Brussels, Belgium

[3] Institute of Epidemiology, Helmholtz Zentrum München, Member of the German Center for Lung Research (DZL), Neuherberg, Germany

[4] Institute of Lung Biology and Disease and Comprehensive Pneumology Center with the CPC-M bioArchive, Helmholtz Zentrum Muenchen, Member of the German Center for Lung Research (DZL), Munich, Germany.

[5] Department of Medicine V, University Hospital, LMU, Member of the German Center for Lung Research (DZL), Munich, Germany

[6] Dept. of Pneumology, Teaching Hospital Pyhrn-Eisenwurzen Klinikum Steyr, Austria

[7] Research Unit Protein Science, Metabolomics and Proteomics Core, Helmholtz Zentrum München, Munich, Germany

Correspondence to:

Silke Meiners, PhD

Comprehensive Pneumology Center, Max-Lebsche-Platz 31, 81377 München, Germany

Phone: 0049 89 3187 4673

Fax: 0049 89 3187 194673

E-mail: silke.meiners@helmholtz-muenchen.de

We here demonstrate distinct activation of immunoproteasomes in peripheral blood cells of young smokers and COPD patients. Specific inhibition of the immunoproteasome might represent a novel therapeutic concept for COPD treatment.

Author contributions: IEK, SH and SM conception and design of research; MF, KM, AK and CP, JB provided (clinical) samples and reagents; IEK, SH, YW, AU, JP, performed experiments; IEK, SH, YW, OV, SMH, JMP, CF and SM analyzed data; IEK, SH, HS and SM interpreted results; IEK, CF prepared tables and figures; IEK, SH, CF, HS and SM drafted manuscript; IEK and SM edited and revised manuscript; all authors approved final version.

Grants: The research described in this manuscript was funded by the Helmholtz Zentrum München and the Else-Kröner Fresenius Stiftung (2016_A22). Sophie Hardy was funded by the Belgian Respiratory Society and the German Academic Exchange Service and the Université catholique de Louvain (ERASMUS grant). Yuqin Wang was funded by the Chinese Guangzhou Elite Scholarship Council.

ABSTRACT

Immune cells contain a specialized type of proteasome, i.e. the immunoproteasome, which is required for intracellular protein degradation. Immunoproteasomes are key regulators of immune cell differentiation, inflammatory activation and autoimmunity. Immunoproteasome function in peripheral immune cells might be altered by smoking and in COPD thereby affecting immune cell responses.

We here analyzed the expression and activity of proteasome complexes in peripheral blood mononuclear cells (PBMC) isolated from healthy male young smokers as well as from patients with severe COPD and compared them to matching controls. Proteasome expression was upregulated in COPD patients as assessed by RT-qPCR and mass spectrometry-based proteomics analysis. Proteasome activity was quantified using activity-based probes and native gel analysis. We observed distinct activation of immunoproteasomes in the peripheral blood cells of young male smokers and severely ill COPD patients. Native gel analysis and linear regression modeling confirmed robust activation and elevated assembly of 20S proteasomes, which correlated significantly with reduced lung function parameters in COPD patients. The immunoproteasome was distinctly activated in COPD patients upon inflammatory cytokine stimulation of PBMCs *in vitro*. Inhibition of the immunoproteasome reduced proinflammatory cytokine expression in COPD-derived blood immune cells.

Given the crucial role of chronic inflammatory signalling and the emerging involvement of autoimmune responses in COPD, therapeutic targeting of the immunoproteasome might represent a novel therapeutic concept for COPD.

Word count: **** (3691)

Key words: immunoproteasome, COPD, inflammation, cigarette smoke, immunoproteasome inhibitor

INTRODUCTION

Chronic obstructive pulmonary disease (COPD) is a major chronic lung disease estimated to become the third leading cause of death worldwide in 2030 [1]. Notably, there is a lack of innovative therapies for this disease. Cigarette smoke is the main risk factor for the development of COPD [2]. It causes oxidative stress that damages DNA and proteins [3], results in degradation and remodeling of lung tissue and initiates innate and adaptive immune dysfunction driving COPD disease development [4, 5].

The ubiquitin-proteasome system is the main protein degradation pathway in the cell. The proteasome hydrolyses most cellular proteins including short-lived cellular regulators such as transcription factors, cell cycle and signalling molecules into small peptides [6, 7]. Degradation products are used for amino acid recycling and as major histocompatibility complex (MHC) class I antigens enabling immune surveillance by $CD8^+$ T cells [8, 9]. The most prominent proteasome complexes are the 26S and the 20S core proteasomes with the 26S consisting of the 20S catalytic core and one or two 19S regulators (Figure 1A) [7]. Immune cells contain a specialized type of proteasome, i.e. the immunoproteasome, harbouring the three distinct catalytic subunits LMP2, MECL-1 and LMP7 [8, 9]. Immunoproteasomes are key regulators of immune cell activation and differentiation [9, 10]. In particular, they play a major role in inflammatory signalling by regulating activation of inflammatory transcription factors such as NFκB [11]. Specific inhibition of the immunoproteasome counteracts autoimmunity and inflammatory immune responses [12, 13]

We and others have previously demonstrated that lung tissue proteasomes are inhibited by cigarette smoke resulting in accumulation of oxidatively damaged proteins and altered MHC class I antigen presentation [14–17]. Proteasome activity in lung tissue of end-stage COPD patients is severely impaired [16, 18] and protein aggregates accumulate in COPD lungs [19].

These data indicate that proteasome function and proteostasis in lungs of COPD patients is severely disturbed possibly contributing to the exacerbation of disease, altered MHC class I antigen presentation and susceptibility to virus infections [16, 20].

In this study, we extended our understanding of proteasome function in COPD by focussing on the analysis of the proteasome in peripheral blood immune cells of young male smokers and COPD patients. We here demonstrate distinct activation of immune cell proteasomes in smokers and severely ill COPD patients.

METHODS

Further details on the methods, primers and antibodies used in this study can be found in the supplement.

Human samples: For the first study arm, EDTA-blood samples of 20 young, self-reported healthy never-smokers and 20 current smoking subjects were obtained (Table 1). We chose male participants to exclude any potential hormonal variations. Inclusion criteria were male gender, age between 20 and 30 years, BMI between 18 and 30, at least 10 cigarettes per day within the last year or never smoking, exclusion criteria were chronic diseases, long-term medication or infectious disease within the last three weeks. Cotinine was assayed in blood plasma via ELISA according to the manufacturer's recommendations (Calbiotech, Cotinine ELISA CO096D) to confirm current smoking status.

For the second arm, analysis was performed in EDTA-blood samples from 30 stable COPD patients (no exacerbation of the disease since at least 6 weeks) and 24 healthy age-matched control subjects were collected from the clinics of the Ludwig-Maximilians-University (LMU) and the outpatient unit of the Comprehensive Pneumology Center (CPC) (Table 2). We also obtained blood samples for our *in vitro* stimulation experiments from there (Supplemental Table S1).

All donors gave written consent. The study was approved by the ethics committee of the medical faculty of the LMU (study number 382-10).

Peripheral blood mononuclear cells (PBMCs) were isolated using Lymphoprep™ and SepMate™ tubes according to the manufacturer's instructions and stored in aliquots at -80°C until analysis. Flow cytometry of full EDTA-blood was performed as detailed in the supplement.

Activity-based probe labeling: Native protein lysates were extracted from PBMCs with 50 mM Tris HCl, pH 7.5, 2 mM DTT, 5 mM $MgCl_2$, 10 % Glycerol, 2 mM ATP, 0.05 % digitonin, cOmplete™ protease inhibitor (Roche). Activity of catalytic subunits was monitored by using activity-based probes (ABP) as described [21].

Native gel analysis and substrate overlay: Native gel analysis and subsequent immunoblotting with an antibody detecting the 20S α1-7 subunits (ab22674, Abcam, Cambridge, UK) was performed as described [22].

PBMC *in vitro* stimulation: Isolated PBMCs were plated in 24 well plates (2x10^6 cells/well), cultivated in RPMI medium (containing 10% FBS (Biochrom) and 100 U/ml Pen/Strep) and treated with or without 75 U/ml of IFNγ (Roche) or LPS (1 µg/ml, Sigma) for 24 h. PMBCs were harvested and RNA or proteins were extracted. Immunoproteasome inhibitor LU-005i was kindly provided by Hermen Overkleeft [23]. 2 hours before LPS stimulation, cells were treated with 0.5 µM LU-005i.

Luminescent activity assay: Chymotrypsin-, caspase- and trypsin-like activities were measured with the Proteasome-Glo™ Assay kit according to the manufacturer's protocol (Promega) and described [24].

Statistics & Software: All analyses were performed using the statistical software package R, version 4.0.3 [25]. Details on the data transformation and regression models are given in the supplement. Outliers exceeding mean ± 4 SD were excluded from the analyses. Differences between groups (non-smoker *vs.* smoker and control *vs.* COPD) were tested using Fisher's exact test for categorical variables and Mann–Whitney–Wilcoxon rank sum test or Kruskal-Wallis rank sum test for continuous variables. Reference equations for spirometry according to the Global Lung function Initiative (GLI) [26] were applied to calculate percent predicted

values of the lung function parameter FEV1/FVC. A *p*-value below 0.05 was used to indicate statistical significance.

RESULTS

To study immunoproteasome function in peripheral blood in detail, we used a two-armed study design reflecting the extremes of the control and disease groups: The first arm included analysis of healthy male current smokers and never-smokers aged 20-30 years (Table 1), the second arm contained mainly end-stage COPD patients and lung healthy controls aged 47-84 years including 16 never and 2 former and 6 current smokers (Table 2). The control groups were not overlapping, and age matched to the respective study arms.

Activation of immunoproteasome in peripheral blood cells of young smokers

The first study arm evaluated the effect of cigarette smoke exposure on proteasome function in peripheral blood mononuclear cells (PBMCs) of young male smokers (Table 1). Current tobacco smoking was confirmed by elevated levels of the metabolic by-product of nicotine, cotinine, in the blood plasma of smokers (Table 1). Flow cytometry analysis of blood cells revealed a significant increase in the absolute number of all analyzed immune cell types in smokers compared to the never-smoking control group (Supplemental Figure S1A). The relative cellular composition of monocytes and leukocytes, however, was not altered between smokers and non-smokers (Supplemental Figure S1B, Supplemental Table S2). Proteasome activity of blood mononuclear cells was analyzed using two distinct methods. First, we assessed the number of active standard and immunoproteasome complexes using specific activity-based probes (ABPs) [27]. These ABPs covalently bind to and label catalytically active proteasome subunits which are then identified according to their molecular weight in denaturing SDS gels [27]. A set of three ABPs was used to differentiate the three standard catalytic subunits of the proteasome β1, β2, and β5 and the immunoproteasome sites LMP2, MECL-1 and LMP7 (Figure 1B). ABP-labeling confirmed that the immunoproteasome is the predominant type of proteasome in PBMCs (Figure 2A) [28].

The catalytic activity in PBMCs was largely preserved upon tobacco smoke consumption (Figure 2A). The β5 activity was almost below detection level in isolated PBMCs as described before (Figure 2A) [29]. In a second approach, we dissected the different proteasome complexes, namely the 26S and the free 20S proteasomes, using native gel analysis. With this method, the proteasome complexes maintain their activity and can be resolved according to their size [22]. The enzymatic activity of the proteasome complexes was quantified by in-gel degradation of a fluorescently quenched substrate for the chymotrypsin-like activity of the proteasome. Of note, 20S proteasome activity was slightly reduced in smokers compared to never-smokers, while 26S and total proteasome activity were not altered (Figure 2B, Supplemental Figure S2A). This shift in activities between 20S and 26S proteasome complexes increased the ratio of 26S to 20S activity in smokers (Figure 2B). Blotting of the native gels and immunodetection of the 20S catalytic core allowed us to quantify the amount of proteasome complexes in the PBMC samples [22]. The abundance of 20S and 26S proteasome complexes was not different between the two groups (Supplemental Figure S2A). By calculating the ratio of activity and abundance, we determined the specific activity of distinct proteasome complexes. The specific activity of the 26S proteasome was significantly elevated in smokers compared to non-smokers (Figure 2B) suggesting that the 26S proteasomes are more active in peripheral blood cells of young healthy smokers. As the overall number of active sites of the proteasome was not grossly altered - as determined by our ABP analysis (Figure 2A) - these data suggest that tobacco smoke exposure in healthy individuals does not increase the expression and amount of proteasome complexes but rather activates the enzymatic activity of the 26S proteasome in the peripheral blood cells. This notion is supported by the comparable RNA expression of

multiple proteasomal subunits of the 26S proteasome in PBMCs of smokers and never-smoking males (Supplemental Figure S2B, Supplemental Table S2).

Immunoproteasome activation in peripheral immune cells of COPD patients

For our second study arm, we applied native gel proteasome activity profiling to analyze proteasome activity in PBMCs isolated from patients with severe COPD (mainly GOLD Stage IV/D) and compared the results to lung healthy age-matched controls (Table 2). Of note, we observed substantial activation of the 20S and total proteasome activity in COPD patients (Figure 3 and Supplemental Figure S3A). In addition, the abundance of all proteasome complexes was increased, indicating elevated assembly of both 20S and 26S proteasome complexes in blood immune cells of COPD patients (Figure 3). The specific activity (activity/abundance) of the 26S proteasome complex and of total proteasomes, however, was significantly reduced in COPD patients (Figure 3). The ratio of the two complexes was not altered (Supplemental Figure S3B). Increased abundance of immune cell proteasome complexes in COPD patients was confirmed by RNA and protein expression analysis: mRNA expression of several proteasome subunits such as the immunoproteasomal genes PSMB9 (encoding LMP7) and PSMB10 (encoding MECL-1), the 19S regulatory subunits PSMC3 and PSMD11 was significantly elevated in COPD PBMCs (Figure 4A). Moreover, mass-spectrometry-based protein analysis of PBMCs revealed concerted upregulation of multiple proteasome subunits in COPD patients compared to controls (Figure 4B). These expression data thus support the observation that COPD patients assemble more proteasome complexes in their peripheral immune cells, which might be part of an adaptive response to compensate for diminished specific 26S proteasome activity.

Robust activation of 20S immunoproteasomes correlates with reduced lung function in COPD

To determine whether the changes in proteasome complexes correlate with altered lung function of COPD patients, we performed correlation analyses for proteasome function and FEV1/FVC impairment (Figure 5A and Supplemental Figure S3C). Of note, we observed a statistically significant negative correlation of 20S activity as well as 20S, 26S and total abundance with FEV1/FVC percent predicted while the specific 26S and total activities correlated positively with this lung function parameter (Figure 5A). These data indicate that patients with severe lung function alterations have higher levels of both 20S and 26S proteasome complexes in their PBMCs. This is associated with a higher activity of 20S immunoproteasomes but not of 26S proteasome complexes. Rather contrary, the 26S and total specific activities, i.e. the activity per complex, are higher in blood immune cells of patients with better lung function. These data demonstrate a complex change in immunoproteasome function in peripheral immune cells of COPD patients, which correlates with the degree of lung function impairment.

Altered immunoproteasome activity might be caused by the skewed immune cell composition in the blood of COPD patients. Our flow cytometry analysis revealed an elevated percentage of granulocytes and monocytes but not lymphocytes in our COPD study cohort (Supplemental Figure S4A, Supplemental Table S3). These latter two cell types represent the main immune cells present in our PBMC isolates (Supplemental Figure S4B). Extracted data from the ImmProt data base [28] and our own preliminary RNA analysis of sorted blood immune cells (data not shown) indicated that proteasomal protein abundance (copy number) is quite similar in lymphocytes, NK, pDCs and monocytes at baseline and does not grossly diverge upon immune cell activation (Supplemental Figure S5). These data

suggest that the amount of proteasomes is rather similar and stable in different immune cell subsets and might thus not be the underlying cause for the observed changes in proteasome activity in COPD patients. We further validated our data by linear regression modeling where we adjusted for multiple parameters of our study cohort such as age, sex, body mass index (BMI), comorbidities as well as differential blood composition and immunosuppressive medication (Figures 5B-C, Suppl. Supplemental Table S4). Of note, these various parameters did not affect the significant activation of 20S activity and 20S abundance as well as activation of total proteasome activity in blood leukocytes of COPD patients (Figure 5C). Moreover, we performed sensitivity analysis on the effect of the 8 ever-smokers in our control groups. As evident from Supplemental Table S5, there is no major change in the beta estimator and the overall alterations in immunoproteasome function are similar. Activation of the 20S proteasome in peripheral immune cells can thus be regarded as a robust feature of patients with severe COPD and unrelated to the smoking status. In contrast, 26S proteasome function appears to be less robust and regulated by additional factors (model 6). This finding requires further analysis.

Inflammatory immunoproteasome regulation in COPD patients

To further investigate whether the activation of the immune cell proteasomes in COPD patients extends to activated immune cells, we challenged freshly isolated PBMC samples from healthy donors and severe COPD patients (Supplemental Table S1) with the inflammatory stimuli interferon γ (IFNγ) or LPS for 24 hours and analyzed proteasome activity. We tested for the three main activities of the proteasome, namely the chymotrypsin -like (CT-L), caspase-like (C-L) and trypsin-like (T-L) proteasome activity, using a luminogenic substrate assay. Of note, all three activities significantly increased in COPD patients upon

stimulation of peripheral blood mononuclear cells with IFNγ (Figure 6A) but were less strongly activated by LPS (Figure 6B) compared to healthy controls. These data demonstrate inflammatory immunoproteasome activation in COPD patients. In an exploratory analysis, we next investigated whether the inhibition of the immunoproteasome affects LPS-induced inflammatory cytokine expression. For that, we pre-treated PBMCs isolated from controls or COPD patients with the specific immunoproteasome inhibitor LU-005i [23] for 2 h before LPS stimulation for 24 h and then assessed inflammatory cytokine expression on the RNA level. After 24 h of LPS stimulation, the immunoproteasome was still effectively inhibited as evidenced both by Western blot-based detection of mass-shifted LMP2 and LMP7 subunits upon covalent binding of the inhibitor (Supplemental Figure 6A) and chemiluminescent activity assays (Supplemental Figure 6B). LPS-induced transcriptional activation of interleukin (IL)-1B, IL6 and IL8 was clearly attenuated by immunoproteasome inhibition, while IL10 was upregulated by immunoproteasome inhibition (Figure 6C). This was most prominent in COPD patients where LPS stimulation strongly activated the expression of these inflammatory cytokines. . These data thus provide first proof-of-concept evidence for a potential beneficial effect of therapeutic immunoproteasome inhibition on inflammatory cytokine expression in COPD.

DISCUSSION

We here show that the proteasome is distinctly activated in peripheral blood cells of young smokers and in patients with severe COPD. Activation of the 20S immunoproteasome correlates with lung function impairment. Moreover, inflammatory stimuli alter immunoproteasome activation in COPD patients and inflammatory cytokine expression is attenuated by immunoproteasome inhibition *in vitro*. This study thus presents first evidence for systemic activation of the immunoproteasome in peripheral blood cells of severely ill COPD patients. Given the key role of the immunoproteasome for immune cell activation and autoimmune responses [9, 12], our data suggest that specific inhibition of the immunoproteasome might represent a novel therapeutic concept for COPD treatment.

Regulation of the immunoproteasome by cigarette smoke and in COPD

We and others previously demonstrated inhibition of the proteasome by cigarette smoke *in vitro*, *in vivo* and in explanted lungs of severely ill COPD patients [14–18]. Impaired protein degradation by the proteasome contributes to the accumulation of damaged proteins and augmented protein stress in lung cells as also demonstrated for neurodegenerative and cardiovascular diseases [30–33].

In this study, we show activation of the immunoproteasome, a specialized type of immune cell proteasome, in peripheral blood cells of healthy young smokers and severely ill COPD patients. Our sophisticated native gel analysis allowed us to dissect proteasome activities of distinct 20S and 26S complexes, which are well known to be differentially regulated [34, 35]. In young smokers, the specific activity of the 26S proteasome was significantly increased while overall proteasome expression and activity were not grossly altered. Activation of the 26S proteasome, which degrades ubiquitinated proteins, might be part of an adaptive

response to adjust proteasome function to an increased protein turnover [34, 36]. This finding is supported by experimental data from chronically smoke-exposed mice, where proteasome activity and expression were increased in the mouse lungs [16, 37].

In peripheral blood cells of COPD patients, however, assembly and activity of the 20S proteasome complexes were activated. Despite the small size of the study population, the effect was robust even when adjusting for various parameters such as sex, age, BMI, comorbidities, differential blood cell count and immunosuppressive medication. Importantly, elevated 20S immunoproteasome activity in the peripheral blood cells of COPD patients correlated significantly with the extent of lung function impairment. These data are well in line with the established concept that the 20S proteasome is activated upon severe oxidative stress to enable ubiquitin-independent degradation of oxidatively modified and damaged proteins [36, 38]. Induction of the immunoproteasome is also part of a conserved protective response to oxidative stress [39, 40]. Increased assembly and activity of the proteasome is most likely due to transcriptional activation as we observed elevated mRNA and protein levels in peripheral immune cells of COPD patients. We cannot rule out, however, that the increased levels of 20S proteasomes also involve disassembly of the 26S proteasome in COPD patients. Dissociation of the 26S into its 19S and 20S subcomplexes takes place in response to oxidative stress [41, 42]. Accordingly, we have previously shown that the 26S proteasome becomes instable in cells and lungs exposed to cigarette smoke [17]. The abundance of 26S proteasome complexes was elevated in COPD patients together with increased protein levels of 19S and 20S subunits. 26S proteasome activity, however, was not equally elevated, but the specific 26S activity was reduced instead. We speculate that 26S assembly is activated as a frustrated attempt of the immune cells to compensate for the loss of 26S proteasome activity in immune cells of COPD patients. The here observed activation

of immunoproteasome function in peripheral blood immune cells is in contrast to the previously described inhibition of proteasome activity in lung tissue of COPD patients. This discrepancy might be resolved by the short-lived nature of peripheral immune cells, which prevents sustained accumulation of oxidative damage but favours acute adaptation to oxidative and inflammatory stress in COPD. Moreover, we speculate that there is an exposure dose or damage-related threshold for proteasome function, which will either allow adaptive activation or detrimental inhibition depending on the duration and extent of damage. This concept accords with homeostatic regulation circuits that are common for cellular stress responses [43] and reflects the complexity of protein quality control in the cell.

Our present study is limited to the analysis of severe cases of COPD but provides first proof-of-concept evidence for disease-related regulation of the immunoproteasome in peripheral blood cells. Of note, altered immunoproteasome activity in blood immune cells of severe COPD patients might represent a potential circulating biomarker for COPD severity, disease progression and exacerbation frequency. The analysis of large cohorts with longitudinal data from COPD patients of different GOLD stages and lung healthy control samples, which we are currently pursuing, will deliver the required statistical power to test our biomarker hypothesis. This approach may also allow us to delineate whether the activation of the immunoproteasome is an epiphenomenon of severe COPD or an early event and related to COPD disease severity.

Therapeutic targeting of the immunoproteasome in COPD

We here describe a novel role for the immunoproteasome in COPD patients. The immunoproteasome was activated in PBMCs isolated from severely ill COPD patients

compared to healthy controls. Moreover, it was further activated upon *ex vivo* stimulation of PBMCs with the inflammatory cytokine IFNγ or LPS. Importantly, inhibition of the immunoproteasome with the specific inhibitor LU-005i attenuated LPS-induced expression of proinflammatory cytokines such as IL1B, IL6 and IL8 from isolated PBMCs *in vitro*. In contrast, expression of IL10 was activated by immunoproteasome inhibition which may contribute to protective immune regulation by this key anti-inflammatory cytokine [44]. One may speculate that therapeutic application of immunoproteasome inhibitors may thus contribute to the restoration of the dysfunctional immune system in COPD. Our data are well in line with studies showing regulation of proinflammatory cytokine secretion such as interleukin IL6, IFNγ, and TNFα upon immunoproteasome inhibition [45–48]. Immunoproteasome function also shapes dendritic cell programs and controls T and B cell differentiation [10]. In particular, immunoproteasome activity is crucial for the differentiation and function of T helper (Th) cell lineages, namely Th1 and Th17 differentiation [49]. Specific inhibition of the immunoproteasome revealed an extended function for immunoproteasomes in autoimmunity with suppression of pro-inflammatory cytokine secretion, plasma cell-mediated antibody production and Th17 differentiation [10, 45, 46, 50]. Accordingly, immunoproteasome inhibitors are currently tested in clinical trials for treatment of autoimmune polymyositis and lupus nephritis (www.clinicaltrials.gov) [12, 13]. Given the crucial role of chronic inflammatory signalling in propagation of COPD as a systemic disease [4, 51], the prominent role of Treg versus Th1/Th17 function [52, 53] and the potential involvement of autoimmune responses in COPD [54], therapeutic targeting of the immunoproteasome might represent a novel therapeutic concept for COPD. Our in vitro data on the reduced activation of inflammatory cytokines from circulating blood mononuclear cells suggest a beneficial systemic effect of immunoproteasome inhibition

which may diminish pro-inflammatory signalling in COPD lungs and attenuate disease progression.

ACKNOWLEDGEMENTS

We gratefully acknowledge the provision of human biomaterial and clinical data from the CPC-M bioArchive and its partners at the Asklepios Biobank Gauting, the Klinikum der Universität München and the Ludwig-Maximilians-Universität München. We are thankful for the excellent support by Patricia Sklarek from the CPC outpatient unit.

REFERENCES

1. Decramer M, Janssens W, Miravitlles M. Chronic obstructive pulmonary disease. *Lancet* 2012; 379: 1341–1351.

2. Postma DS, Bush A, van den Berge M. Risk factors and early origins of chronic obstructive pulmonary disease. *Lancet* 2015; 385: 899–909.

3. Church DF, Pryor WA. Free-radical chemistry of cigarette smoke and its toxicological implications. *Environ. Health Perspect.* 1985; 64: 111–126.

4. Brusselle GG, Joos GF, Bracke KR. New insights into the immunology of chronic obstructive pulmonary disease. *Lancet* 2011; 378: 1015–1026.

5. Caramori G, Casolari P, Barczyk A, Durham AL, Di Stefano A, Adcock I. COPD immunopathology. *Semin. Immunopathol.* 2016; 38: 497–515.

6. Schmidt M, Finley D. Regulation of proteasome activity in health and disease. *Biochim. Biophys. Acta* 2014; 1843: 13–25.

7. Coux O, Zieba BA, Meiners S. The Proteasome System in Health and Disease. *Adv. Exp. Med. Biol.* 2020; 1233: 55–100.

8. Basler M, Kirk CJ, Groettrup M. The immunoproteasome in antigen processing and other immunological functions. *Curr. Opin. Immunol.* 2013; 25: 74–80.

9. Kammerl IE, Meiners S. Proteasome function shapes innate and adaptive immune responses. *Am. J. Physiol. Lung Cell. Mol. Physiol.* 2016; 311: L328-336.

10. Groettrup M, Kirk CJ, Basler M. Proteasomes in immune cells: more than peptide producers? *Nat. Rev. Immunol.* 2010; 10: 73–78.

11. Beling A, Kespohl M. Proteasomal Protein Degradation: Adaptation of Cellular Proteolysis With Impact on Virus-and Cytokine-Mediated Damage of Heart Tissue During Myocarditis. *Front. Immunol.* 2018; 9: 2620.

12. Basler M, Mundt S, Bitzer A, Schmidt C, Groettrup M. The immunoproteasome: a novel drug target for autoimmune diseases. *Clin. Exp. Rheumatol.* 2015; 33: 74–79.

13. Ettari R, Zappalà M, Grasso S, Musolino C, Innao V, Allegra A. Immunoproteasome-selective and non-selective inhibitors: A promising approach for the treatment of multiple myeloma. *Pharmacol. Ther.* 2018; 182: 176–192.

14. van Rijt SH, Keller IE, John G, Kohse K, Yildirim AÖ, Eickelberg O, Meiners S. Acute cigarette smoke exposure impairs proteasome function in the lung. *Am. J. Physiol. Lung Cell. Mol. Physiol.* 2012; 303: L814-823.

15. Somborac-Bacura A, van der Toorn M, Franciosi L, Slebos D-J, Zanic-Grubisic T, Bischoff R, van Oosterhout AJM. Cigarette smoke induces endoplasmic reticulum stress response and proteasomal dysfunction in human alveolar epithelial cells. *Exp. Physiol.* 2013; 98: 316–325.

16. Kammerl IE, Dann A, Mossina A, Brech D, Lukas C, Vosyka O, Nathan P, Conlon TM, Wagner DE, Overkleeft HS, Prasse A, Rosas IO, Straub T, Krauss-Etschmann S, Königshoff M, Preissler G, Winter H, Lindner M, Hatz R, Behr J, Heinzelmann K, Yildirim AÖ, Noessner E, Eickelberg O, Meiners S. Impairment of Immunoproteasome Function by Cigarette Smoke and in Chronic Obstructive Pulmonary Disease. *Am. J. Respir. Crit. Care Med.* 2016; 193: 1230–1241.

17. Kammerl IE, Caniard A, Merl-Pham J, Ben-Nissan G, Mayr CH, Mossina A, Geerlof A, Eickelberg O, Hauck SM, Sharon M, Meiners S. Dissecting the molecular effects of cigarette smoke on proteasome function. *J. Proteomics* 2019; 193: 1–9.

18. Baker TA, Bach HH, Gamelli RL, Love RB, Majetschak M. Proteasomes in lungs from organ donors and patients with end-stage pulmonary diseases. *Physiol. Res. Acad. Sci. Bohemoslov.* 2014; 63: 311–319.

19. Min T, Bodas M, Mazur S, Vij N. Critical role of proteostasis-imbalance in pathogenesis of COPD and severe emphysema. *J. Mol. Med. Berl. Ger.* 2011; 89: 577–593.

20. Donnelly LE. Could Protecting the Immunoproteasome Reduce Exacerbations in Chronic Obstructive Pulmonary Disease? *Am. J. Respir. Crit. Care Med.* 2016; 193: 1188–1190.

21. Keller IE, Vosyka O, Takenaka S, Kloß A, Dahlmann B, Willems LI, Verdoes M, Overkleeft HS, Marcos E, Adnot S, Hauck SM, Ruppert C, Günther A, Herold S, Ohno S, Adler H, Eickelberg O, Meiners S. Regulation of immunoproteasome function in the lung. *Sci. Rep.* 2015; 5: 10230.

22. Yazgili AS, Meul T, Welk V, Semren N, Kammerl IE, Meiners S. In-gel proteasome assay to determine the activity, amount, and composition of proteasome complexes from mammalian cells or tissues. *STAR Protoc.* 2021; 2: 100526.

23. de Bruin G, Huber EM, Xin B-T, van Rooden EJ, Al-Ayed K, Kim KB, Kisselev AF, Driessen C, van der Stelt M, van der Marel G a, Groll M, Overkleeft HS. Structure-based design of either β1i or β5i specific inhibitors of human immunoproteasomes. *J. Med. Chem.* 2014; 57: 6197-209.

24. Welk V, Coux O, Kleene V, Abeza C, Trümbach D, Eickelberg O, Meiners S. Inhibition of Proteasome Activity Induces Formation of Alternative Proteasome Complexes. *J. Biol. Chem.* 2016; 291: 13147–13159.

25. R Core Team. R: A Language and Environment for Statistical Computing. Vienna, Austria; 2020. Available from: https://www.R-project.org/. .

26. Quanjer PH, Stanojevic S, Cole TJ, Baur X, Hall GL, Culver BH, Enright PL, Hankinson JL, Ip MSM, Zheng J, Stocks J, ERS Global Lung Function Initiative. Multi-ethnic reference values for spirometry for the 3-95-yr age range: the global lung function 2012 equations. *Eur. Respir. J.* 2012; 40: 1324–1343.

27. de Bruin G, Xin BT, Kraus M, van der Stelt M, van der Marel GA, Kisselev AF, Driessen C, Florea BI, Overkleeft HS. A Set of Activity-Based Probes to Visualize Human (Immuno)proteasome Activities. *Angew. Chem. Int. Ed Engl.* 2016; 55: 4199–4203.

28. Rieckmann JC, Geiger R, Hornburg D, Wolf T, Kveler K, Jarrossay D, Sallusto F, Shen-Orr SS, Lanzavecchia A, Mann M, Meissner F. Social network architecture of human immune cells unveiled by quantitative proteomics. *Nat. Immunol.* 2017; 18: 583–593.

29. Schmidt C, Berger T, Groettrup M, Basler M. Immunoproteasome Inhibition Impairs T and B Cell Activation by Restraining ERK Signaling and Proteostasis. *Front. Immunol.* 2018; 9: 2386.

30. Powers ET, Morimoto RI, Dillin A, Kelly JW, Balch WE. Biological and chemical approaches to diseases of proteostasis deficiency. *Annu. Rev. Biochem.* 2009; 78: 959–991.

31. Bouchecareilh M, Balch WE. Proteostasis: a new therapeutic paradigm for pulmonary disease. *Proc. Am. Thorac. Soc.* 2011; 8: 189–195.

32. Meiners S, Eickelberg O. What shall we do with the damaged proteins in lung disease? Ask the proteasome! *Eur. Respir. J.* 2012; 40: 1260–1268.

33. Wei J, Rahman S, Ayaub EA, Dickhout JG, Ask K. Protein misfolding and endoplasmic reticulum stress in chronic lung disease. *Chest* 2013; 143: 1098–1105.

34. Rousseau A, Bertolotti A. Regulation of proteasome assembly and activity in health and disease. *Nat. Rev. Mol. Cell Biol.* 2018; 19: 697–712.

35. VerPlank JJS, Lokireddy S, Zhao J, Goldberg AL. 26S Proteasomes are rapidly activated by diverse hormones and physiological states that raise cAMP and cause Rpn6 phosphorylation. *Proc. Natl. Acad. Sci. U. S. A.* 2019; 116: 4228–4237.

36. Wang X, Meul T, Meiners S. Exploring the proteasome system: A novel concept of proteasome inhibition and regulation. *Pharmacol. Ther.* 2020; 211: 107526.

37. Conlon TM, John-Schuster G, Heide D, Pfister D, Lehmann M, Hu Y, Ertüz Z, Lopez MA, Ansari M, Strunz M, Mayr C, Angelidis I, Ciminieri C, Costa R, Kohlhepp MS, Guillot A, Günes G, Jeridi A, Funk MC, Beroshvili G, Prokosch S, Hetzer J, Verleden SE, Alsafadi H, Lindner M, Burgstaller G, Becker L, Irmler M, Dudek M, Janzen J, et al. Inhibition of LTβR signalling

activates WNT-induced regeneration in lung. *Nature* 2020; 588: 151–156.

38. Kumar Deshmukh F, Yaffe D, Olshina MA, Ben-Nissan G, Sharon M. The Contribution of the 20S Proteasome to Proteostasis. *Biomolecules* 2019; 9.

39. Pickering AM, Koop AL, Teoh CY, Ermak G, Grune T, Davies KJA. The immunoproteasome, the 20S proteasome and the PA28αβ proteasome regulator are oxidative-stress-adaptive proteolytic complexes. *Biochem. J.* 2010; 432: 585–594.

40. Seifert U, Bialy LP, Ebstein F, Bech-Otschir D, Voigt A, Schröter F, Prozorovski T, Lange N, Steffen J, Rieger M, Kuckelkorn U, Aktas O, Kloetzel P-M, Krüger E. Immunoproteasomes preserve protein homeostasis upon interferon-induced oxidative stress. *Cell* 2010; 142: 613–624.

41. Wang X, Yen J, Kaiser P, Huang L. Regulation of the 26S proteasome complex during oxidative stress. *Sci. Signal.* 2010; 3: ra88.

42. Livnat-Levanon N, Kevei E, Kleifeld O, Krutauz D, Segref A, Rinaldi T, Erpapazoglou Z, Cohen M, Reis N, Hoppe T, Glickman MH. Reversible 26S Proteasome Disassembly upon Mitochondrial Stress. *Cell Rep.* 2014; 7: 1371–1380.

43. Martins I, Galluzzi L, Kroemer G. Hormesis, cell death and aging. *Aging* 2011; 3: 821–828.

44. Ouyang W, Rutz S, Crellin NK, Valdez PA, Hymowitz SG. Regulation and Functions of the IL-10 Family of Cytokines in Inflammation and Disease. *Annu. Rev. Immunol.* 2011; 29: 71–109.

45. Muchamuel T, Basler M, Aujay MA, Suzuki E, Kalim KW, Lauer C, Sylvain C, Ring ER, Shields J, Jiang J, Shwonek P, Parlati F, Demo SD, Bennett MK, Kirk CJ, Groettrup M. A selective inhibitor of the immunoproteasome subunit LMP7 blocks cytokine production and attenuates progression of experimental arthritis. *Nat. Med.* 2009; 15: 781–787.

46. Basler M, Mundt S, Muchamuel T, Moll C, Jiang J, Groettrup M, Kirk CJ. Inhibition of the immunoproteasome ameliorates experimental autoimmune encephalomyelitis. *EMBO Mol. Med.* 2014; 6: 226–238.

47. Basler M, Claus M, Klawitter M, Goebel H, Groettrup M. Immunoproteasome Inhibition Selectively Kills Human CD14 + Monocytes and as a Result Dampens IL-23 Secretion. *J. Immunol.* 2019; : ji1900182.

48. Santos RDLA, Bai L, Singh PK, Murakami N, Fan H, Zhan W, Zhu Y, Jiang X, Zhang K, Assker JP, Nathan CF, Li H, Azzi J, Lin G. Structure of human immunoproteasome with a reversible and noncompetitive inhibitor that selectively inhibits activated lymphocytes. *Nat. Commun.* Springer US; 2017; 8: 1–10.

49. Kalim KW, Basler M, Kirk CJ, Groettrup M. Immunoproteasome Subunit LMP7 Deficiency and Inhibition Suppresses Th1 and Th17 but Enhances Regulatory T Cell Differentiation. *J. Immunol. Baltim. Md 1950* 2012; 189: 4182–4193.

50. Huber EM, Basler M, Schwab R, Heinemeyer W, Kirk CJ, Groettrup M, Groll M. Immuno- and constitutive proteasome crystal structures reveal differences in substrate and inhibitor specificity. *Cell* 2012; 148: 727–738.

51. Brightling C, Greening N. Airway inflammation in COPD: progress to precision medicine. *Eur. Respir. J.* 2019; 54.

52. Le Rouzic O, Pichavant M, Frealle E, Guillon A, Si-Tahar M, Gosset P. Th17 cytokines: novel potential therapeutic targets for COPD pathogenesis and exacerbations. *Eur. Respir. J.* 2017; 50.

53. Xu W, Li R, Sun Y. Increased IFN-γ-producing Th17/Th1 cells and their association with lung function and current smoking status in patients with chronic obstructive pulmonary disease. *BMC Pulm. Med.* 2019; 19: 137.

54. Scambler T, Holbrook J, Savic S, McDermott MF, Peckham D. Autoinflammatory disease in the lung. *Immunology* 2018; .

FIGURE LEGENDS

FIGURE 1: Overview on the analysis of proteasome complexes in this study. (A) The 26S proteasome complex consists of a central 20S core particle capped with one or two 19S regulatory particles. The 20S particle consists of four rings with seven subunits each, two outer α-rings and two inner β-rings, where the three proteolytically active subunits reside: β1, β2, and β5 constitute the standard proteasome, the three immunosubunits LMP2, MECL-1 and LMP7 can be induced e.g. by IFNγ, but are constitutively expressed at high levels in immune cells. **(B)** Nomenclature of gene and protein names, enzymatic activity and activity-based probe (ABP) used to differentiate immune- and standard proteasome.

FIGURE 2: Proteasome activity profiling in peripheral blood mononuclear cells (PBMC) of young healthy smokers and non-smokers. (A) Activity-based probe (ABP) analysis of proteasome activity in PBMCs of smokers (n=20) and non-smokers (n=18-19) with signal quantification (labeling intensity) using the pan-reactive MV151, the β5 and LMP7-specific MVB127, and the β1 and LMP2 specific LW124 ABP. All samples were run on one large gel to allow direct comparison of signals. **(B)** Native gel analysis of native protein lysates of PBMCs of smokers (S) (n=20) and non-smokers (NS) (n=19) with fluorescent activity assay for the chymotrypsin-like (CT-L) activity of the proteasome. Subsequent immunoblotting of the native gels using an antibody against the α1-7 subunits of the 20S catalytic core was applied to quantify proteasome complex abundance. Densitometry analysis of the gels is shown for the activities as relative signal intensity. Samples were run on 4 different gels and each sample was normalized to mean intensity of the controls. The specific activity is defined as activity/abundance, specifically, the activity signal of the 20S, 26S or sum of both (total activity) divided by the densitometric signal for immunostaining, i.e. abundance of the

respective complex. Statistical analysis: median ± quartile, whiskers indicate the range. Mann-Whitney-U-Test, * = $p<0.05$, ** = $p<0.01$.

FIGURE 3: **Proteasome activity in peripheral blood mononuclear cells (PBMC) of healthy control subjects and COPD patients.** Native gel analysis of PBMC native protein lysates of healthy control subjects (n=15, 9 never/2 former/4 current smokers) and COPD patients (n=12) with fluorescent activity assay for the chymotrypsin-like (CT-L) activity of the proteasome and subsequent immunoblotting of the native gel using an antibody against the α1-7 subunits for detection of proteasome complex abundance (see Supplementary Figure S3A). Samples were run on 4 different gels and each sample was normalized to mean intensity of the controls. Densitometry analysis of the gels is shown as normalized signal to the mean of the controls. The specific activity is given as the ratio of activity per abundance. Statistical analysis: median ± quartile, whiskers indicate the range. Mann-Whitney-U-Test, * = $p<0.05$, ** = $p<0.01$, *** = $p<0.001$.

FIGURE 4: Profiling of proteasome expression in peripheral blood mononuclear cells (PBMC) of healthy control subjects and COPD patients. (A) RT-qPCR analysis of the α-subunit PSMA3, immunoproteasome subunits PSMB8-10 and 19S subunits PSMC3 and PSMD11 in PBMCs of healthy controls (n=21-22) and COPD patients (n=27-29). RPL19 and HPRT were used as housekeeping genes. Fold change over control is shown. **(B)** Mass spectrometry analysis of total proteins in PBMCs of COPD (n=10) and controls (n=10) with a heatmap of all 20S (PSMA and PSMB) and 19S subunits (PSMC and PSMD). Significantly upregulated subunits are marked in bold red, downregulated ones in bold blue. Statistical analysis: median ± quartile, whiskers indicate the range. Mann-Whitney-U-Test, * = $p<0.05$,

** = $p<0.01$.

FIGURE 5: Correlation and linear regression analysis of proteasome complex with selected clinical parameters. (A) Spearman correlations of lung function (FEV1/FVC %pred) with the proteasome complex parameters activity, abundance and specific activity (activity/abundance). Significant correlations are highlighted in bold blue (negative correlation) and bold red (positive correlation). **(B)** and **(C)** Parameters of the proteasome complex analysis were adjusted for sex, age, and BMI (Model 2), additionally comorbidities and % granulocytes (Model 3), % lymphocytes (Model 4) or the number of leukocytes per µl blood (Model 5) and also for immunosuppressive medication (Model 6). Model 1 shows the unadjusted values. Data were standardized prior to calculation of the regression coefficient β (with 95% confidence interval). Significant regression estimates are depicted in black, non-significant are depicted in grey. See also Supplemental Table S4 for the corresponding values. Abbreviations: BMI, body mass index; comorb., comorbidities; immunosuppr., immunosuppressive; n.s., not significant; %pred., percent predicted according to GLI [26]; spec., specific.

FIGURE 6: Alterations on proteasome activities upon IFNγ- or LPS-treatment of PBMCs isolated from healthy controls and COPD patients. PBMCs of healthy controls (n=6-14) and COPD patients (n=6-10) were treated with **(A)** 75 U/ml IFNγ or **(B)** 1 µg/ml LPS for 24 h. Proteasome chymotrypsin-like (CT-L), caspase-like (C-L) and trypsin-like (T-L) activities were analyzed using chemiluminescent substrates specific for the respective activities and are shown as fold over the respective untreated control. **(C)** mRNA expression of cytokines IL1B, IL6, IL8 and IL10 were measured in PBMCs of healthy controls (n=9) or COPD patients (n=7)

treated with the immunoproteasome inhibitor LU-005i (0.5 µM, 2 h pre-treatment) and/or LPS (1 µg/ml, 24 h). RPL19 and HPRT were used as housekeeping genes. Displayed is the fold change over solvent control in the control and COPD groups and with all samples combined (Comb). Statistical analysis: A and B: median ± quartile, whiskers indicate the range. One sample Wilcoxon test, * = $p<0.05$, ** = $p<0.01$. C: Paired t-test within groups, * = $p<0.05$, Mann-Whitney-U test for difference between LPS-treated control and COPD groups, ## = $p<0.01$, ### = $p<0.001$.

Table 1: Study population of young healthy male smokers and non-smokers

	Never-Smoker		Smoker		*p*-value[B]
	% or median (range)	n/N or N	% or median (range)	n/N or N	
allergies					
no	90	18/20	95	19/20	
yes	10	2/20	5	1/20	1.000
pack years	NA	20	3.5 (1.5; 10.0)	20	NA
age, years	24 (18; 30)	20	24.5 (19; 29)	20	0.978
BMI[A], kg/m²	22.70 (18.59; 27.45)	20	23,27 (19.60; 28.60)	20	0.387
Cotinine (ng/ml)	0.88 (0.62-1.28)	20	314.2 (142.6-693.6)	20	**<0.001**

[A] Body Mass Index

[B] Differences between groups were tested using Fisher's exact test for categorical variables and Wilcoxon rank sum test for continuous variables

Table 2: Study population of lung healthy controls and COPD patients

	Never Smoking Control		Ever Smoking Control		COPD		*p*-value[E]
	% or median (range)	n/N or N	% or median (range)	n/N or N	% or median (range)	n/N or N	
sex							
female	62.50	10/16	75.00	6/8	53.33	16/30	
male	37.50	6/16	25.00	2/8	46.67	14/30	0.550
age, years	56 (47; 64)	16	54.5 (48; 58)	8	60 (47; 84)	29	**0.006**
BMI[A], kg/m²	23.53 (20.07; 33.43)	15	25.82 (20.76; 32.00)	8	22.45 (17.18; 32.00)	28	0.258
comorbidities[B]							
no	81.25	13/16	62.50	5/8	73.33	22/30	
yes	18.75	3/16	37.50	3/8	26.67	8/30	0.571
immunosuppressive medication[C]							
no	100.00	15/15	100.00	8/8	57.14	16/28	
yes	0.00	0/15	0.00	0/8	42.86	12/28	**0.001**
smoking status							
current	0.00	0/16	75.00	6/8	0.00	0/30	
former	0.00	0/16	25.00	2/8	96.67	29/30	
never	100.00	16/16	0.00	0/8	3.33	1/30	**<0.001**

A

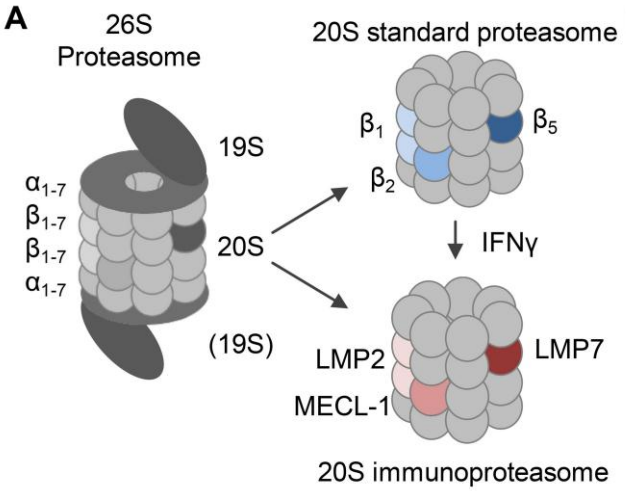

B

Gene	Protein	Activity	
		enzyme	ABP
PSMB6	β1	Caspase-like (C-L)	LW124
PSMB9	LMP2		
PSMB7	β2	Trypsin-like (T-L)	MV151
PSMB10	MECL-1		
PSMB5	β5	Chymotrypsin-like (CT-L)	MVB127
PSMB8	LMP7		

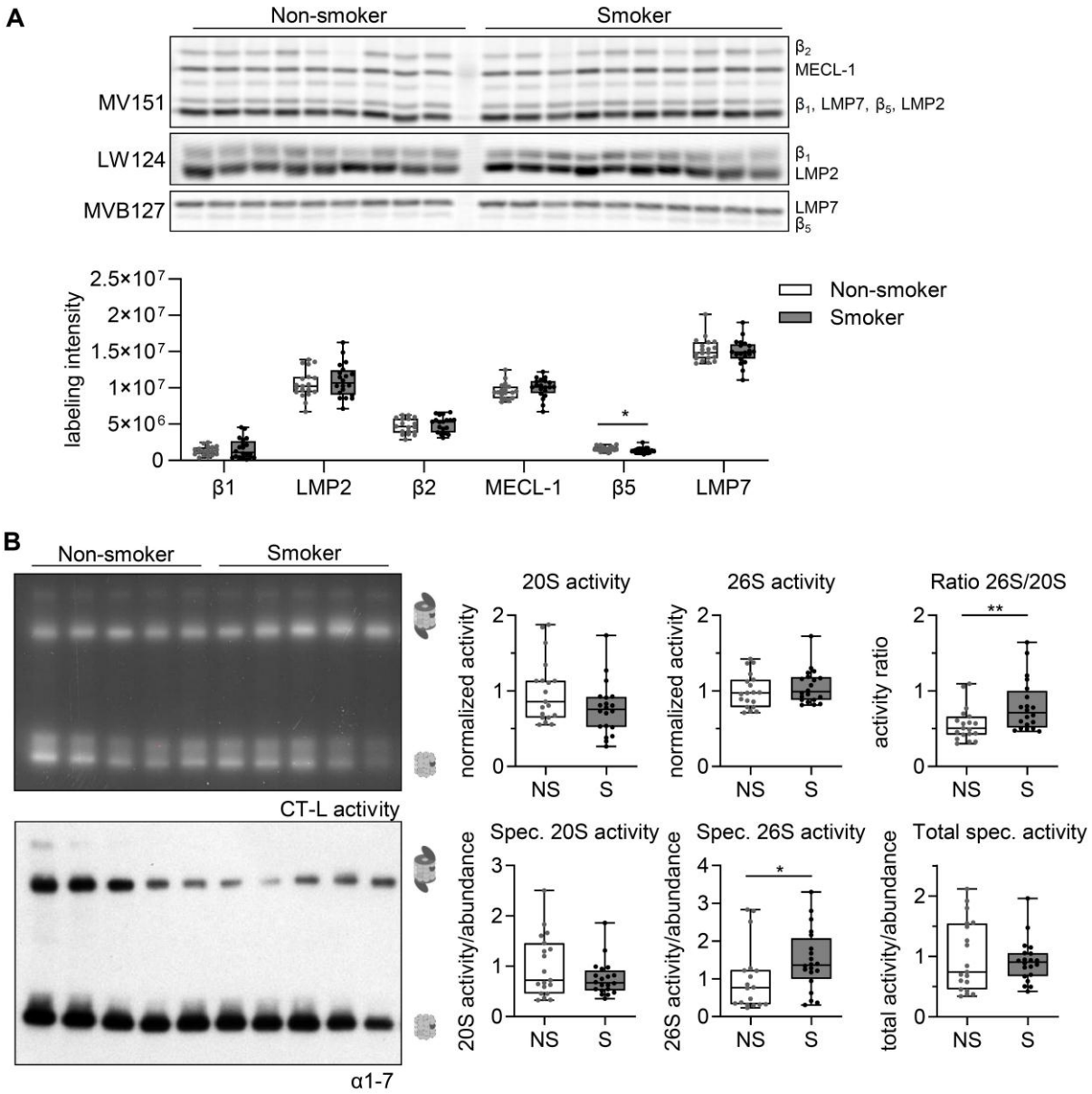
A
Non-smoker
Smoker
MV151
LW124
MVB127
β2
MECL-1
β1, LMP7, β5, LMP2
β1
LMP2
LMP7
β5
labeling intensity
2.5×10^7
2×10^7
1.5×10^7
1×10^7
5×10^6
0
Non-smoker
Smoker
*
β1
LMP2
β2
MECL-1
β5
LMP7
B
Non-smoker
Smoker
CT-L activity
α1-7
20S activity
normalized activity
NS
S
26S activity
normalized activity
NS
S
Ratio 26S/20S
activity ratio
**
NS
S
Spec. 20S activity
20S activity/abundance
NS
S
Spec. 26S activity
26S activity/abundance
*
NS
S
Total spec. activity
total activity/abundance
NS
S

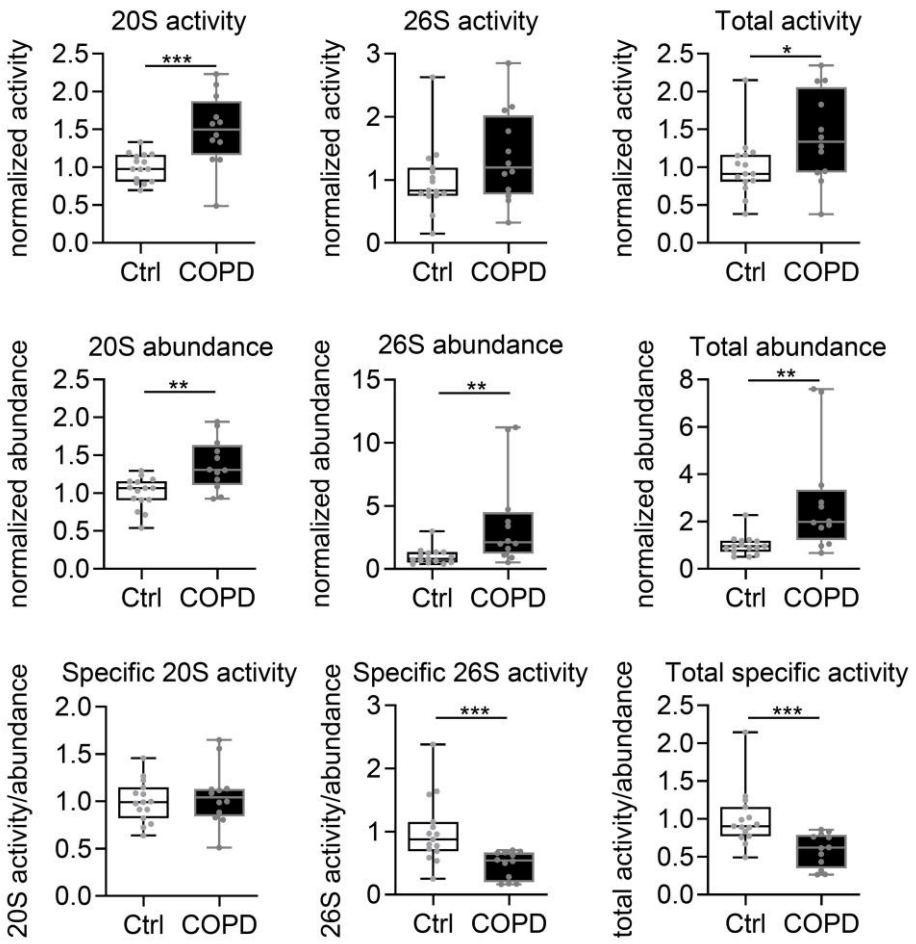
20S activity
normalized activity
***
Ctrl
COPD
26S activity
normalized activity
Ctrl
COPD
Total activity
normalized activity
*
Ctrl
COPD
20S abundance
normalized abundance
**
Ctrl
COPD
26S abundance
normalized abundance
**
Ctrl
COPD
Total abundance
normalized abundance
**
Ctrl
COPD
Specific 20S activity
20S activity/abundance
Ctrl
COPD
Specific 26S activity
26S activity/abundance
***
Ctrl
COPD
Total specific activity
total activity/abundance
***
Ctrl
COPD

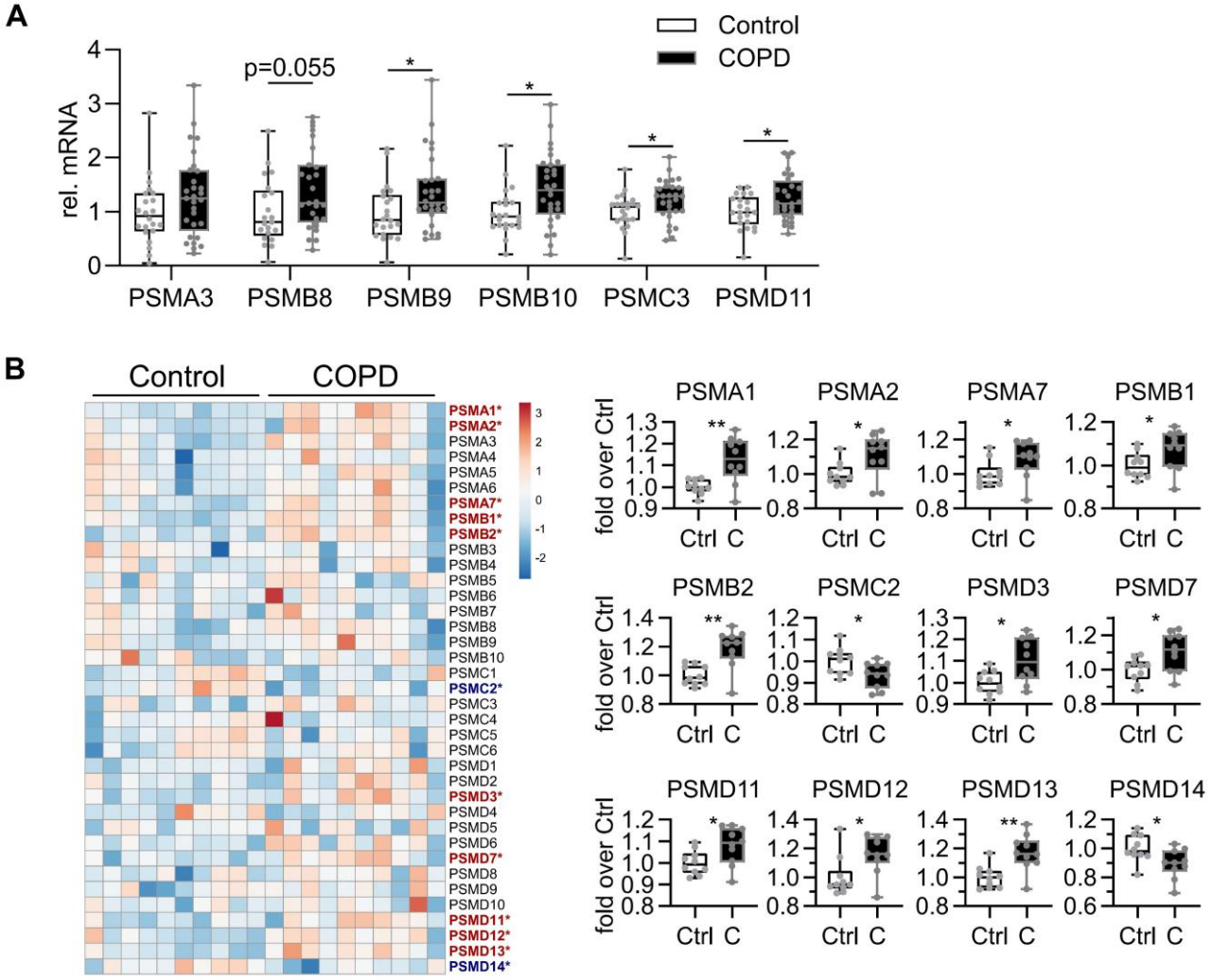
A
Control
COPD
rel. mRNA
p=0.055
PSMA3
PSMB8
PSMB9
PSMB10
PSMC3
PSMD11
B
Control
COPD
PSMA1*
PSMA2*
PSMA3
PSMA4
PSMA5
PSMA6
PSMA7*
PSMB1*
PSMB2*
PSMB3
PSMB4
PSMB5
PSMB6
PSMB7
PSMB8
PSMB9
PSMB10
PSMC1
PSMC2*
PSMC3
PSMC4
PSMC5
PSMC6
PSMD1
PSMD2
PSMD3*
PSMD4
PSMD5
PSMD6
PSMD7*
PSMD8
PSMD9
PSMD10
PSMD11*
PSMD12*
PSMD13*
PSMD14*
PSMA1
PSMA2
PSMA7
PSMB1
PSMB2
PSMC2
PSMD3
PSMD7
PSMD11
PSMD12
PSMD13
PSMD14
fold over Ctrl
Ctrl
C

A

	Spearman ρ FEV1/FVC (%pred)	*p*-value
20S activity	**-0.482**	0.020
26S activity	-0.131	n.s.
Total activity	-0.275	n.s.
26S/20S ratio	0.243	n.s.
20S abundance	**-0.485**	0.019
26S abundance	**-0.462**	0.026
Total abundance	**-0.464**	0.026
spec. 20S activity	-0.008	n.s.
Spec. 26S activity	**0.508**	0.013
Tot. spec. activity	**0.479**	0.021

B

Model	Adjustments
1	unadjusted
2	sex, age and BMI
3	Model 2 + comorb. and % granulocytes
4	Model 2 + comorb. and % lymphocytes
5	Model 2 + comorb. and leukocytes
6	Model 5 + immunosuppr. medication

C

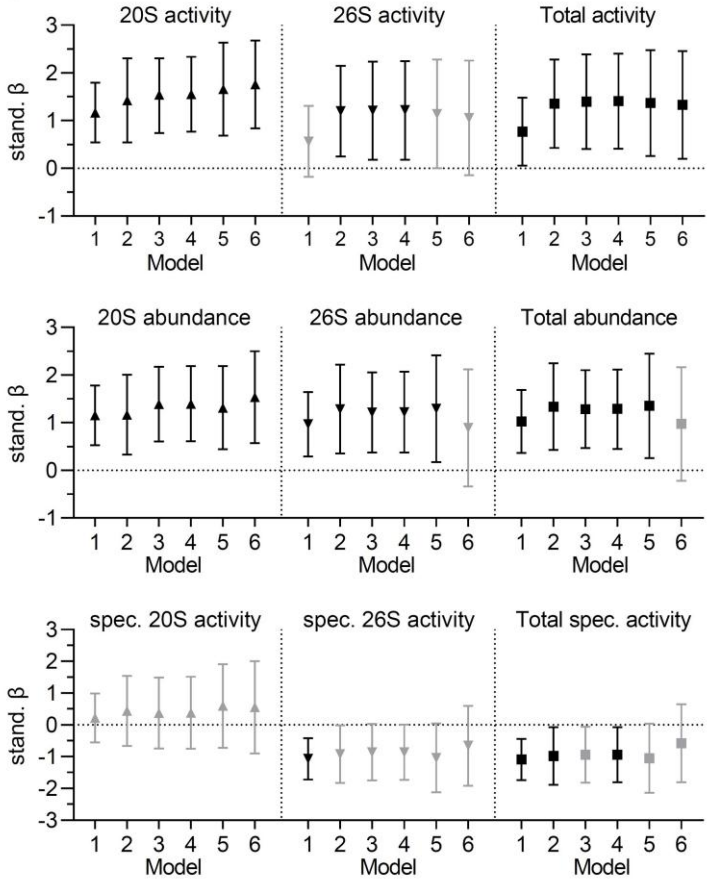

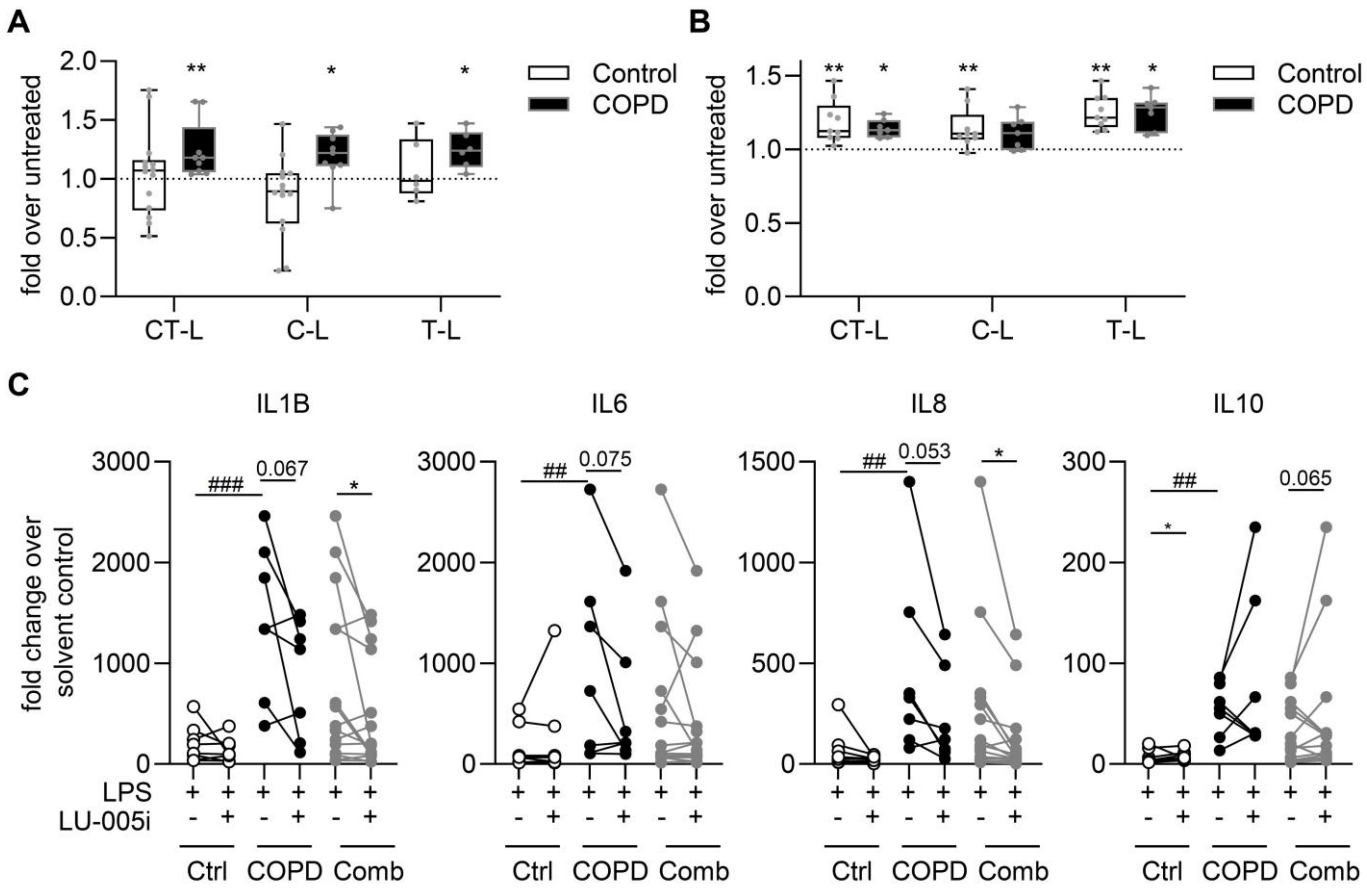
A
fold over untreated
2.0
1.5
1.0
0.5
0.0
**
*
*
CT-L
C-L
T-L
Control
COPD
B
fold over untreated
1.5
1.0
0.5
0.0
**
*
**
**
*
CT-L
C-L
T-L
Control
COPD
C
IL1B
IL6
IL8
IL10
fold change over solvent control
3000
2000
1000
0
###
0.067
*
##
0.075
1500
500
0.053
300
200
100
0.065
LPS
LU-005i
Ctrl
COPD
Comb

Online Data Supplement

Activation of immune cell proteasomes in peripheral blood of smokers and COPD patients - implications for therapy

Ilona E. Kammerl, Sophie Hardy, Claudia Flexeder, Andrea Urmann, Julia Peierl, Oliver Vosyka, Yuqin Wang, Marion Frankenberger, Katrin Milger-Kneidinger, Jürgen Behr, Andrea Koch, Juliane Merl-Pham, Stefanie M. Hauck, Charles Pilette, Holger Schulz, Silke Meiners

SUPPLEMENTARY METHODS

Quantitative real-time RT-PCR: Total RNA from cells was isolated using Roti®-Quick-Kit (Carl Roth, Karlsruhe, Germany), reverse transcribed using random hexamers (Life Technologies) and MMLV reverse transcriptase (Sigma-Aldrich). Quantitative PCR was performed using the SYBR Green LC480 System as described before [1] (Roche Diagnostics, Mannheim, Germany), gene-specific primer sequences are listed below.

Primer sequences

Target Gene	Forward (5'-3')	Reverse (5'-3')
HPRT	TGAAGGAGATGGGAGGCCA	AATCCAGCAGGTCAGCAAAGAA
RPL19	TGTACCTGAAGGTGAAGGGG	GCGTGCTTCCTTGGTCTTAG
PSMA3	AGATGGTGTTGTCTTTGGGG	AACGAGCATCTGCCAACAA
PSMB5	TCAGTGATGGTCTGAGCCTG	CCATGGTGCCTAGCAGGTAT
PSMB6	CAGAACAACCACTGGGTCCT	CCCGGTATCGGTAACACATC
PSMB7	TCGCTGGGGTGGTCTATAAG	TCCCAGCACCACAACAATAA
PSMB8	GTTCCAGCATGGAGTGATTG	TTGTTCACCCGTAAGGCACT
PSMB9	ATGCTGACTCGACAGCCTTT	GCAATAGCGTCTGTGGTGAA
PSMB10	AGCCCGTGAAGAGGTCTGG	CATAGCCTGCACAGTTTCCTCC
PSMC3	GTGAAGGCCATGGAGGTAGA	GTTGGATCCCCAAGTTCTCA
PSMD11	GCTCAACACCCCAGAAGATGT	AGCCTGAGCCACGCATTTTA

Flow cytometry analysis: Flow cytometry was used to quantify the different leukocyte populations in the blood of non-smokers, smokers, COPD patients and controls. 100 µl of EDTA-blood was mixed with fluorescently labeled antibodies (see table below) in flow cytometry tubes and then incubated at 4°C for 20 minutes in the dark. After incubation, erythrocytes were lysed with the Q-Prep Workstation (Beckman Coulter). 100 µl flow count fluorospheres (Beckman Coulter) were added to the samples right before measurement. Samples were run on a LSR II flow cytometer and data were analyzed using BD FACSDiva Software Version 8.0 (Becton Dickinson). In the forward scatter/side scatter analysis the three main leukocyte populations can be identified: granulocytes, monocytes and

lymphocytes. Then, to specify the cell types, the following antigens were used: CD15 and CD16 for neutrophilic granulocytes (CD15, CD16), eosinophilic granulocytes (CD15), monocytes (CD14, CD16), T cells (CD3), natural killer cells (CD16, CD56), B cells (CD19). To validate the specificity of the antibodies, each one was compared to an isotype control with the same fluorophore. Cell numbers were calculated using the known concentration of flow count fluorospheres or were given as % of the total cell count (sum of granulocytes, monocytes and lymphocytes).

Antibodies for FACS

Antibody	Fluorophore	Cat. Number	Clone	Manufacturer	Dilution
CD3	Pacific Blue	558117	UCHT1	BD Pharmingen	01:50
IgG1	Pacific Blue	558120	MOPC-21	BD Pharmingen	01:50
CD14	APC	IM2580	RMO52	Beckman Coulter	01:50
IgG2a	APC	A12693	7T4-1F5	Beckman Coulter	01:50
CD15	FITC	562370	W6D3	BD Pharmingen	01:20
IgG1	FITC	555748	MOPC-21	BD Pharmingen	01:20
CD16	PE	A07766	3G8	Beckman Coulter	01:50
IgG1	PE	A07796	679.1Mc7	Beckman Coulter	01:50
CD19	PECy5	555414	HIB19	BD Pharmingen	01:50
IgG1	PECy5	555750	MOPC-21	BD Pharmingen	01:50
CD56	PECy7	557747	B159	BD Pharmingen	01:20
IgG1	PECy7	557872	MOPC-21	BD Pharmingen	01:20

Western blot: Native protein lysates were separated on 15% SDS-gels, blotted onto PVDF membranes and probed with antibodies detecting LMP2 (ab3328, Abcam) and LMP7 (ab3329 Abcam). HRP-coupled secondary antibody (Cell Signaling) and HRP-coupled β-Actin (A3854, clone AC-15, Sigma-Aldrich) were used as described previously [1].

Mass-spectrometry based analysis or PBMC proteins: Each 10 µg of PBMC cell lysate was proteolysed using a modified FASP protocol [2, 3]. Briefly, proteins were reduced and alkylated using dithiothreitol and iodoacetamide, and diluted to 4 M urea prior to

centrifugation on a 30 kDa filter device (PALL or Sartorius). After several washing steps using 8 M urea and ammoniumbicarbonate, proteins were digested by Lys-C and trypsin. Generated peptides were eluted by centrifugation, acidified with TFA and stored at -20°C.

Samples of 10 COPD patients and 10 controls were measured on a Q-Exactive HF mass spectrometer (Thermo scientific) online coupled to an Ultimate 3000 nano-RSLC (Dionex) in data-independent acquisition mode as described [4, 5] in 37 DIA windows of variable size spanning in total from 300–1650 m/z. The recorded raw files were analysed using the Spectronaut 10 software (Biognosys; [6]) with an in-house human spectral meta library which was generated using Proteome Discoverer 2.1, Byonic search engine (Protein Metrics) and the Swissprot human database (release 2017_02). Identifications were filtered for a maximum peptide false discovery rate of 1%. Quantification was based on the sum of MS2 area levels of all unique peptides per protein with the q value percentile 0.25 setting. Again, resulting protein abundances were exported and used for calculation of fold-changes and unpaired significance values.

Proteasome subunits PSMA1-7, PSMB1-10 (20S subunits) as well as PSMC1-6, PSMD1-14 (19S subunits) were displayed using the ClustVis webtool (https://biit.cs.ut.ee/clustvis/) [7].

Statistics

Proteasome parameters were transformed to have mean 0 and standard deviation 1. Linear regression models were used to analyze the association between disease status (control *vs.* COPD and non-smoker *vs.* smoker) and proteasome parameters. Six models with different adjustment were calculated for all proteasome parameters:

- Model 1 was unadjusted,
- Model 2 was adjusted for sex, age and BMI,

- Model 3 was adjusted for all variables included in Model 2 and additionally for percentage granulocytes and comorbidities (defined as diabetes, stroke, myocardial infarction and/or hypertension)
- Model 4 was adjusted for all variables in Model 2 and additionally for percentage lymphocytes and comorbidities.
- Model 5 was adjusted as in Model 2 plus comorbidities and total cell count leukocytes
- Model 6 accounts for all Model 5 parameters and additionally adjusted for immunosuppressive medication. Furthermore, sensitivity analyses with inverse-normal rank transformed proteasome parameters were performed.

SUPPLEMENTARY FIGURES

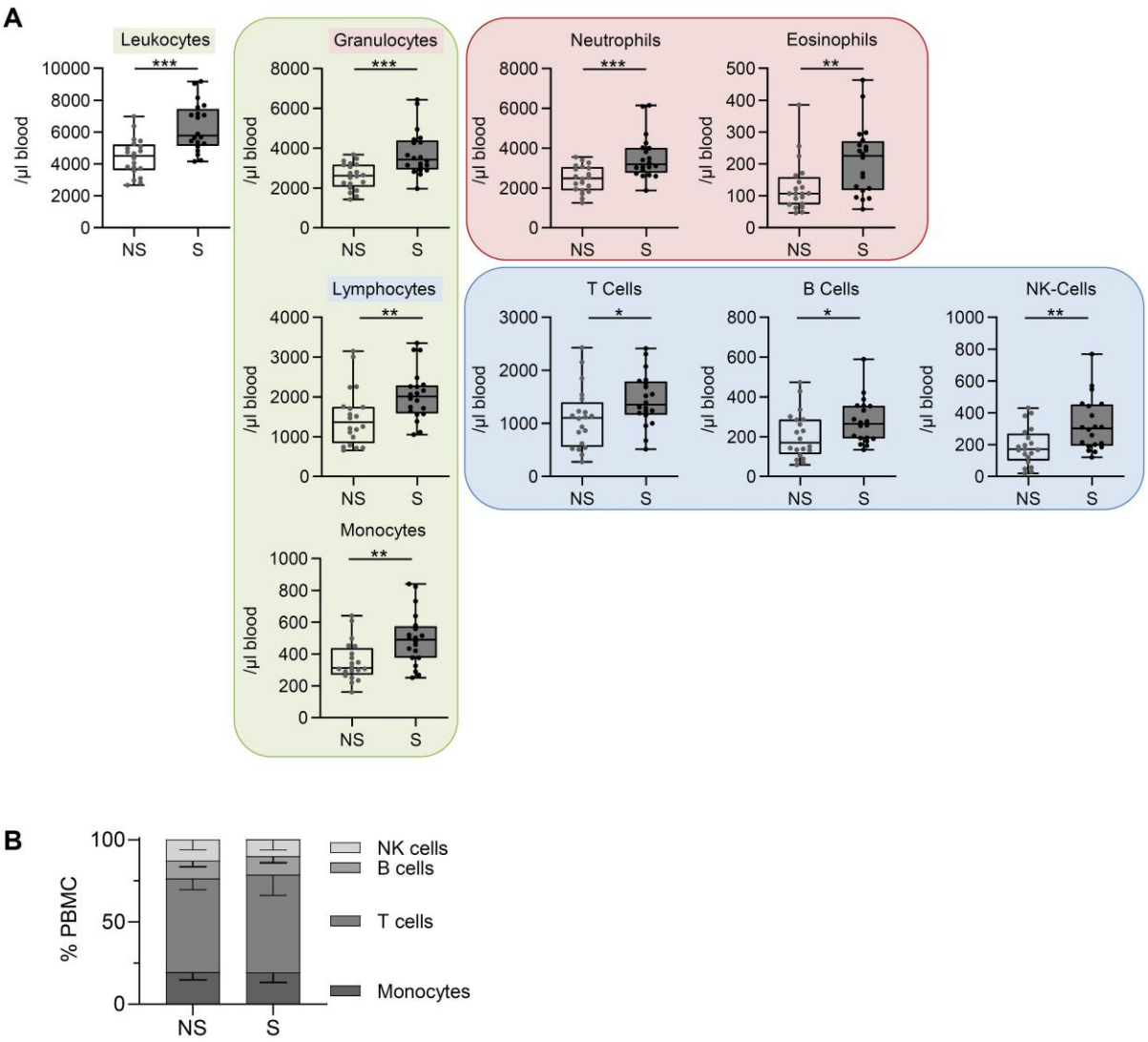

FIGURE S1: Flow cytometry analysis of healthy male smokers and non-smokers. (A) Flow cytometry analysis of PBMCs of smokers (n=20) and never-smokers (n=20). Total leukocytes (cells/µl of blood) and cell numbers of the different populations: granulocytes (subdivided into neutrophils and eosinophils), lymphocytes (subdivided into B cells, T cells, NK cells), and monocytes). **(B)** Distribution of the different blood PBMC subpopulations in smokers and never-smokers (lymphocytes and monocytes). Statistical analysis: (A) median ± quartile, whiskers indicate the range, (B) % of the total number of PBMC + standard deviation. Mann-Whitney-U-Test, * = $p<0.05$, ** = $p<0.01$, *** = $p<0.001$.

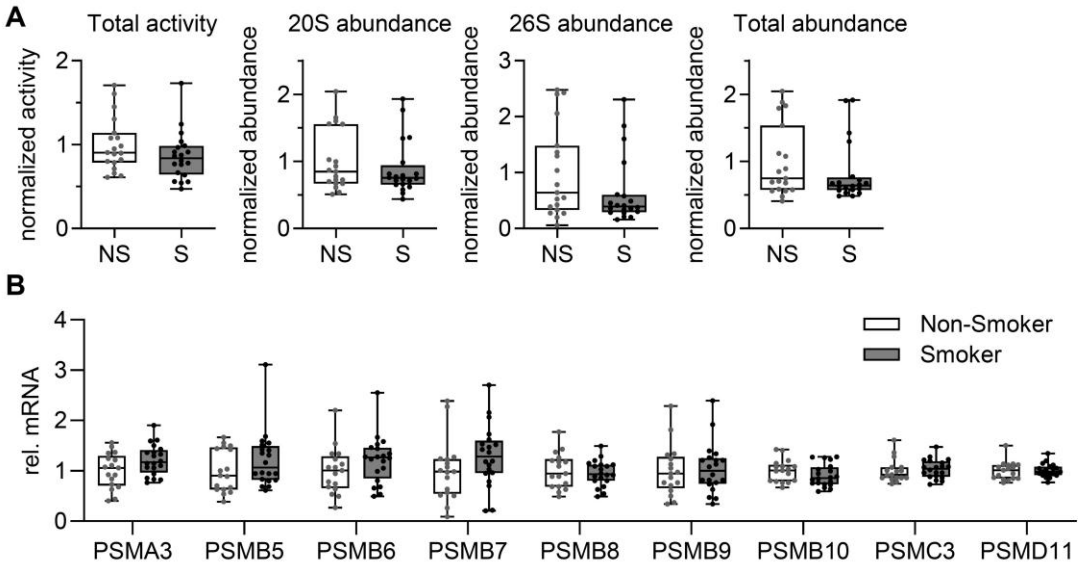

FIGURE S2: Native gel and mRNA analysis of isolated PBMCs of healthy male non-smokers and smokers. (A) 20S and 26S abundance was quantified with the α1-7 antibody upon immunoblotting of the native gels. **(B)** Relative mRNA levels of α-subunit PSMA3, standard proteasome subunits PSMB5-7, immunoproteasome subunits PSMB8-10 and 19S subunits PSMC3 and PSMD11 were evaluated by RT-qPCR in PBMCs of healthy non-smokers (n=17) and smokers (n=20). Data are normalized to the mean of control values, displayed are median ± quartile, whiskers indicate the range.

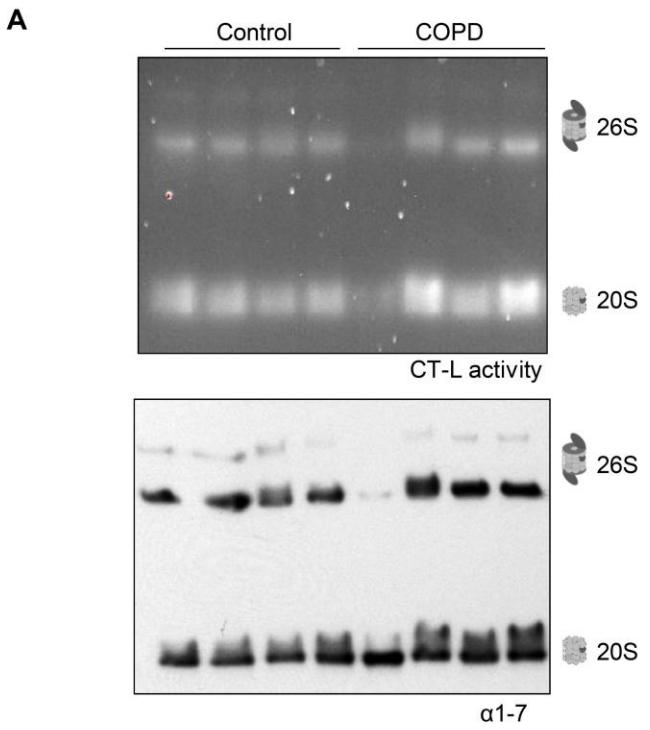

C

		activity				abundance			spec. activity		
		20S	26S	Total	26S/20S	20S	26S	Total	20S	26S	Total
FEV1/FVC	ρ	-0.449	-0.064	-0.209	0.298	-0.413	-0.428	-0.436	-0.014	0.541	0.503
	p-value	0.028	n.s.	n.s.	n.s.	0.045	0.037	0.033	n.s.	0.006	0.012
FEV1/FVC (%pred)	ρ	-0.482	-0.131	-0.275	0.243	-0.485	-0.462	-0.464	-0.008	0.508	0.479
	p-value	0.020	n.s.	n.s.	n.s.	0.019	0.026	0.026	n.s.	0.013	0.021

ρ 1 0 -1

FIGURE S3: Representative native gel with proteasome activity analysis and immunoblotting used in Figure 3 and correlations of native gel parameters with lung function. (A) Representative native gel of control and COPD samples with fluorescent activity assay for the chymotrypsin-like (CT-L) activity of the proteasome and subsequent immunoblotting of the native gel for detection of proteasome complex abundance using an antibody against the α1-7 subunits of the 20S catalytic core. **(B)** Ratio of 26S to 20S activity in control (n=15) and COPD patients (n=12). **(C)** Spearman correlation coefficient and *p*-value of native gel and lung function parameters from 27 samples. Significant correlation coefficients are depicted in colour: red for positive and blue for negative correlation. Abbreviations: n.s., not significant; %pred., percent predicted value according to GLI [8]; spec., specific.

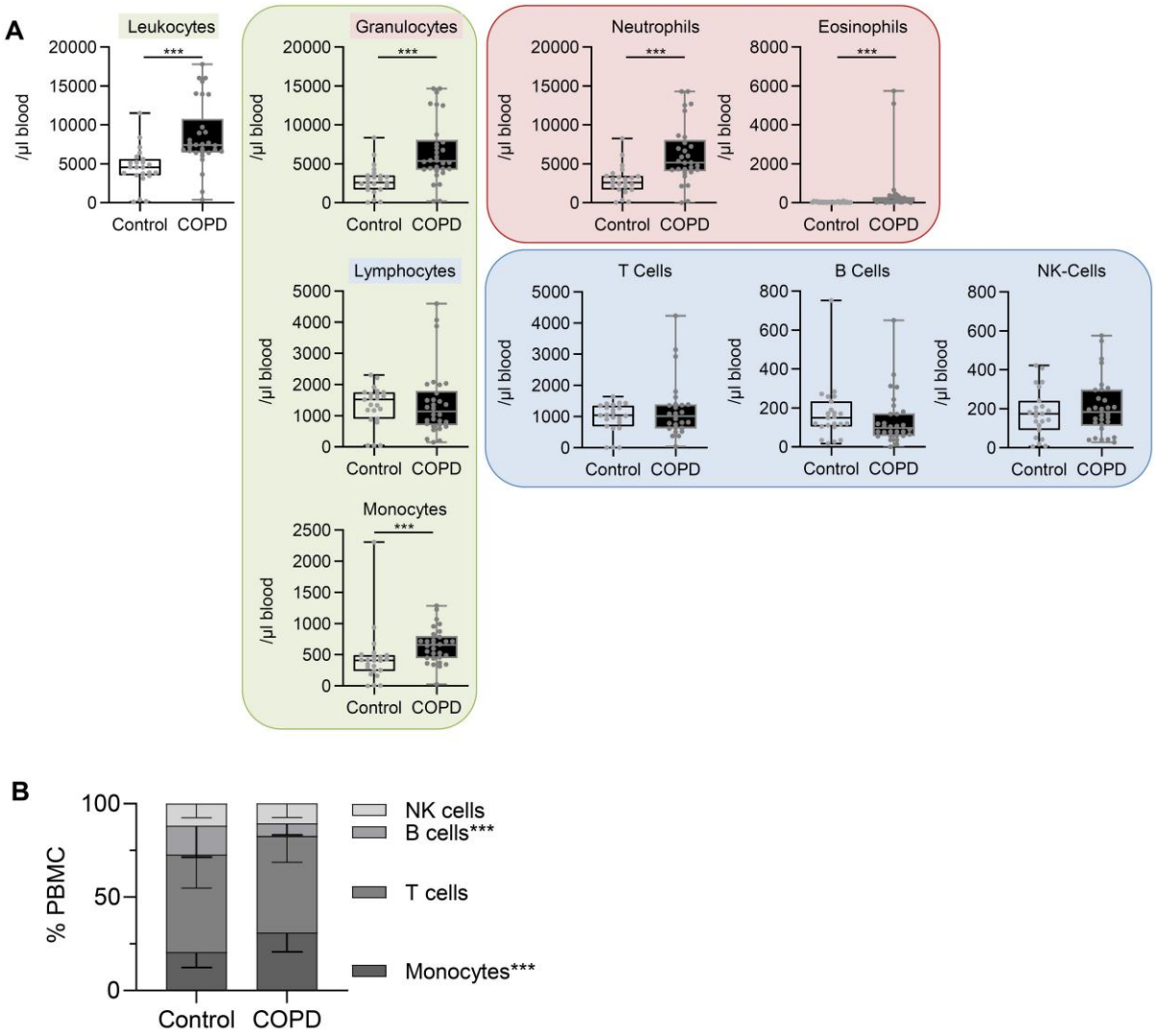

FIGURE S4: Flow cytometry analysis of blood immune cells of healthy controls and COPD patients. (A) Flow cytometry analysis of blood isolated from healthy controls (n=23) and COPD patients (n=29-30). Total leukocytes (cells/µl of blood) and cell numbers of the different populations: granulocytes (subdivided into neutrophils and eosinophils), lymphocytes (subdivided into B cells, T cells, NK cells), and monocytes). **(B)** Distribution of the different blood PBMC subpopulations in controls and COPD patients (lymphocytes and monocytes). Statistical analysis: (A) median ± quartile, whiskers indicate the range, (B) % of the total number of PBMC + standard deviation. Mann-Whitney-U-Test, *** = p<0.001.

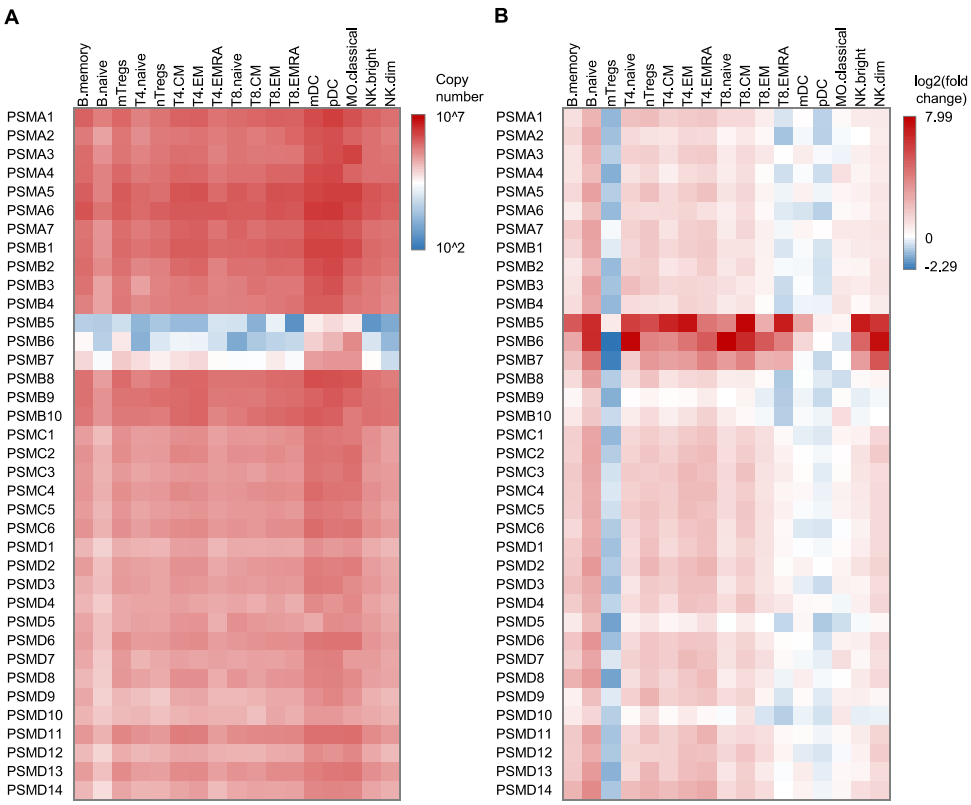

FIGURE S5: Protein levels of proteasome subunits in distinct immune cell types at baseline and upon cell activation. (A) Data extracted from the public database Immprot (www.immprot.org, [9]) where the authors used high-resolution mass spectrometry-based proteomics to characterize 28 primary human hematopoietic cell populations in steady and activated states at a depth of > 10,000 proteins in total. Proteins copy numbers (given as a log10 scale) of the different proteasome subunits (20S subunits PSMA/PSMB, 19S subunits PSMC/PSMD) at a steady state in 17 primary human cell populations of PBMCs. **(B)** Relative log2 fold change of protein copy number of the different proteasome subunits (20S subunits PSMA/PSMB, 19S subunits PSMC/PSMD) upon activation of the same cell populations as in (A).

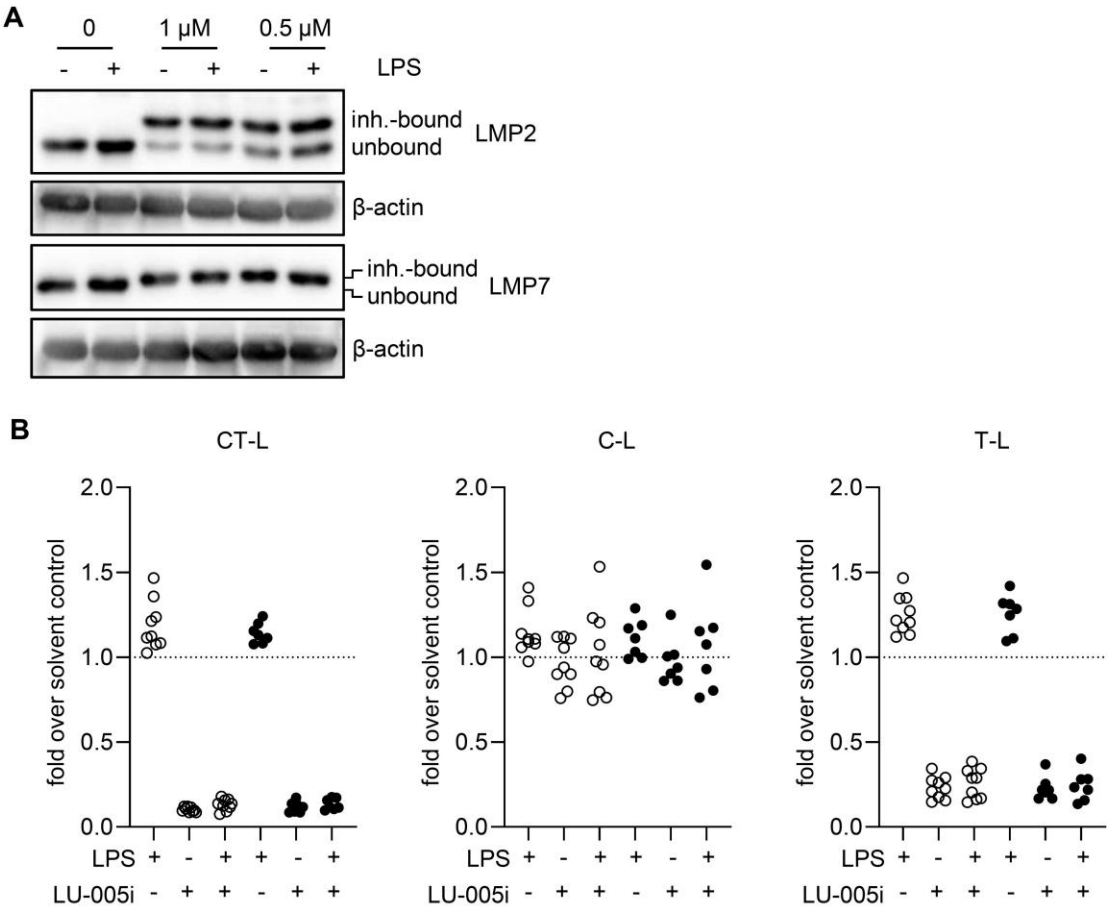

FIGURE S6: Inhibitory profile of LU-005i. (A) PBMCs of a healthy control treated with the immunoproteasome inhibitor LU-005i (1 or 0.5 µM, 2 h pre-treatment) and/or LPS (1 µg/ml, 24 h). Western Blot analysis shows a mass shift of LMP2 and LMP7 immunoproteasome subunits upon inhibitor binding. β-Actin was used as loading control. **(B)** The same samples as in Figure 6C in the main manuscript are shown, which were treated as follows: LU-005i (0.5 µM, 2 h pre-treatment) and/or LPS (1 µg/ml, 24 h). Proteasome chymotrypsin-like (CT-L), caspase-like (C-L) and trypsin-like (T-L) activities were analyzed using chemiluminescent substrates specific for the respective activities and are shown as fold over solvent control set to 1.

SUPPLEMENTARY TABLES

TABLE S1: Study population of lung healthy controls and COPD patients used for *in vitro* stimulations of PBMCs (Figure 6).

	Control		COPD	
	% or median (range)	n/N or N	% or median (range)	n/N or N
sex				
female	64.7	11/17	33.3	6/18
male	35.5	6/17	66.6	12/18
age, years	49 (23-67)		66 (52-81)	
BMI[A], kg/m²	NA		24.21 (15.62-31.28)	
smoking status				
current	11.8	2/17	22.2	4/18
former	0	0/17	55.5	10/18
never	88.2	15/17	22.2	4/18
pack years	NA		35 (10-100)	
GOLD stage				
II/III/IV	NA		2/9/7	
A/B/C/D	NA		2/5/0/11	
FEV1/FVC, %	NA		46.6 (21.0-63.0)	
FEV1/FVC pp GLI, %[B]	NA		59.7 (26.9-81.9))	

[A] Body Mass Index
[B] percent predicted according to GLI [8]

TABLE S2: Overview on the statistical results from the Non-smoker/Smoker cohort

	Non-smoker		Smoker		*p*-value[F]
	% or median (min; max)	N	% or median (min; max)	N	
Flow cytometry					
Granulocyte, %[A]	60.15 (29.67; 73.16)	20	61.99 (44.60; 70.11)	20	0.947
Lymphocyte, %[B]	32.17 (18.80; 62.56)	20	30.37 (23.03; 46.52)	20	0.820
Monocyte, %[C]	7.70 (5.28; 11.54)	20	7.39 (5.23; 10.94)	20	0.758
Granulocyte cell count[D]	2623 (1427; 3673)	20	3433 (1964; 6440)	20	**0.000**
Eosinophil cell count[D]	107 (46; 385)	20	225 (58; 463)	20	**0.009**
Neutrophil cell count[D]	2488 (1256; 3551)	20	3189 (1876; 6146)	20	**0.001**
Lymphocyte cell count[D]	1363 (662; 3152)	20	2011 (1054; 3356)	20	**0.006**
NK cells cell count[D]	171 (20; 430)	20	302 (121; 769)	20	**0.004**
B cells cell count[D]	170 (59; 473)	20	264 (135; 590)	20	**0.038**
T cells cell count[D]	1106 (277; 2427)	20	1352 (515; 2412)	20	**0.023**
Monocyte cell count[D]	313 (161; 640)	20	489 (251; 840)	20	**0.005**
Leucocyte (total) cell count[E]	4508 (2660; 6986)	20	5775 (4148; 9185)	20	**0.000**
ABP					
β1	1284891 (368749; 2497589)	19	1107734 (140364; 4545832)	20	0.989
β2	4586054 (527506; 6243418)	19	5313600 (979062; 6642317)	20	0.550
β5	1510790 (1007648; 2191690)	19	1296755 (832406; 2476711)	20	**0.028**
LMP2	10243187 (6725317; 13885551)	19	10675056 (7142459; 16251874)	20	0.647
MECL-1	9400175 (8042933; 12468418)	19	10112504 (6708296; 12198368)	20	0.134
LMP7	14832066 (13359995; 20114551)	19	14897213 (11090459; 18983501)	20	0.835
LMP2/β1	8.17 (2.88; 26.75)	19	7.20 (2.65; 28.28)	19	0.840
MECL1/β2	2.10 (1.39; 2.95)	18	2.07 (1.42; 6.85)	20	0.851
LMP7/β5	9.82 (6.42; 15.05)	19	11.41 (5.63; 17.63)	20	0.061
Native Gel					
26S Activity	0.97 (0.71; 1.42)	19	0.99 (0.81; 1.72)	20	0.444
20S Activity	0.86 (0.55; 1.88)	19	0.76 (0.27; 1.73)	20	0.101
Total Activity	0.91 (0.61; 1.71)	19	0.84 (0.47; 1.73)	20	0.166
26S/20S Activity	0.51 (0.30; 1.09)	19	0.71 (0.46; 1.64)	20	**0.007**
26S Abundance	0.64 (0.06; 2.48)	19	0.39 (0.16; 2.31)	20	0.149
20S Abundance	0.85 (0.51; 2.04)	19	0.75 (0.44; 1.93)	20	0.396
Total Abundance	0.75 (0.41; 2.05)	19	0.64 (0.49; 1.92)	20	0.247
Spec. 20S Activity	0.72 (0.33; 2.5)	19	0.67 (0.36; 1.86)	20	0.428
Spec. 26S Activity	0.77 (0.23; 2.83)	18	1.37 (0.31; 3.3)	20	**0.024**

	Non-smoker		Smoker		*p*-value[F]
	% or median (min; max)	N	% or median (min; max)	N	
Spec. Total Activity	0.74 (0.34; 2.12)	19	0.91 (0.42; 1.96)	20	0.901
qPCR					
PSMA3	0.13 (0.05; 0.19)	17	0.14 (0.09; 0.23)	20	0.091
PSMB5	0.00 (0.00; 0.00)	17	0.00 (0.00; 0.00)	20	0.253
PSMB6	0.05 (0.01; 0.11)	17	0.06 (0.02; 0.12)	20	0.124
PSMB7	0.09 (0.01; 0.22)	17	0.12 (0.02; 0.25)	20	0.097
PSMB8	0.03 (0.02; 0.06)	17	0.03 (0.02; 0.05)	20	0.726
PSMB9	0.00 (0.00; 0.00)	17	0.00 (0.00; 0.00)	20	0.714
PSMB10	0.94 (0.62; 1.33)	17	0.80 (0.55; 1.19)	20	0.175
PSMC3	0.09 (0.07; 0.16)	17	0.11 (0.07; 0.15)	20	0.336
PSMD11	0.16 (0.12; 0.24)	17	0.16 (0.12; 0.22)	20	0.772

[A] % granulocyte defined as ratio of granulocyte cell count (= sum of neutrophil and eosinophil cell count) and total cell count

[B] % lymphocyte defined as ratio of lymphocyte cell count (= sum of NK cell, B cell and T cell cell count) and total cell count

[C] % monocyte defined as ratio of monocyte cell count and total cell count

[D] cell count per µl blood

[E] total cell count defined as sum of monocytes, neutrophils, eosinophils, NK cells, B cells and T cells

[F] differences between non-smoker and smoker were tested using Wilcoxon rank sum test

TABLE S3: Overview on the statistical results from the Control/COPD cohort

	Control		COPD		*p*-value[B]
	median (min; max)	N	median (min; max)	N	
Flow cytometry					
Granulocyte, %	62.75 (43.12; 84.65)	23	74.84 (15.81; 91.52)	30	**0.006**
Neutrophil, %	61.44 (42.77; 81.81)	23	71.31 (0.07; 91.24)	29	**0.034**
Eosinophil, %	0.50 (0.14; 5.28)	23	1.75 (0.12; 73.75)	30	**0.005**
Lymphocyte, %	29.60 (12.74; 50.03)	23	18.76 (2.62; 60.45)	30	**0.002**
Monocyte, %	7.52 (1.80; 14.18)	23	8.54 (2.47; 31.49)	30	0.286
Granulocyte, /µl	2601 (62; 8342)	23	5358 (203; 14653)	30	**<0.001**
Neutrophil, /µl	2582 (57; 8250)	23	5162 (1; 14289)	29	**<0.001**
Eosinophil, /µl	19 (4; 97)	23	142 (4; 5739)	30	**<0.001**
Lymphocyte, /µl	1520 (43; 2308)	23	1139 (145; 4595)	30	0.404
NK cells, /µl	174 (5; 423)	23	181 (27; 576)	26	0.560
B cells, /µl	150 (17; 752)	23	97 (1; 650)	26	0.125
T cells, /µl	1039 (5; 1640)	23	1010 (38; 4233)	26	0.909
Monocyte, /µl	407 (3; 940)	23	657 (29; 1284)	30	**<0.001**
Leukocyte, /µl[A]	4576 (112; 11498)	23	7418 (377; 17772)	30	**<0.001**
ABP					
β1	0.61 (0.48; 0.75)	22	0.74 (0.51; 1.05)	17	**0.023**
β2	0.18 (0.00; 0.44)	22	0.09 (0.00; 0.66)	17	0.747
β5	0.98 (0.55; 1.54)	22	0.92 (0.62; 1.31)	17	0.440
LMP2	1.48 (0.76; 3.00)	22	1.67 (0.97; 2.86)	17	0.221
MECL-1	0.63 (0.31; 1.10)	22	0.67 (0.25; 1.12)	17	0.624
LMP7	0.96 (0.61; 1.40)	22	0.98 (0.74; 1.34)	17	0.856
Total (MV151)	0.63 (0.41; 0.93)	22	0.65 (0.32; 1.01)	17	0.856
LMP2/β1	0.96 (0.53; 2.08)	22	0.91 (0.44; 1.58)	17	0.967
MECL1/β2	7.41 (4.01; 971.96)	22	15.28 (3.03; 41.44)	16	0.672
LMP7/β5	7.27 (4.47; 13.87)	22	7.80 (4.41; 14.28)	17	0.492
Native Gel					
26S Activity	1.66 (0.30; 5.26)	15	2.39 (0.65; 5.70)	12	0.217
20S Activity	0.98 (0.70; 1.33)	15	1.50 (0.49; 2.23)	12	**<0.001**
Total Activity	2.74 (1.14; 6.45)	15	4.01 (1.14; 7.03)	12	**0.041**
26S Abundance	1.37 (0.69; 5.16)	15	3.68 (0.90; 19.46)	12	**0.002**
20S Abundance	1.07 (0.54; 1.29)	15	1.31 (0.93; 1.94)	12	**0.002**
Total Abundance	2.60 (1.40; 6.22)	15	5.42 (1.82; 20.77)	12	**0.001**
20S spec. Activity	1.02 (0.66; 1.50)	15	1.07 (0.53; 1.70)	12	0.648
26S spec. Activity	1.15 (0.33; 3.13)	15	0.71 (0.22; 0.92)	12	**<0.001**
Total spec. Act.	1.05 (0.58; 2.50)	15	0.72 (0.31; 1.00)	12	**<0.001**
26S/20S Activity	1.71 (0.35; 4.41)	15	1.54 (1.09; 4.27)	12	0.373
qPCR					
PSMA3	0.92 (0.05; 2.82)	22	1.25 (0.23; 3.34)	29	0.127
PSMB5	0.86 (0.08; 2.04)	19	0.87 (0.14; 3.39)	27	0.808

	Control		COPD		*p*-value[B]
	median (min; max)	N	median (min; max)	N	
PSMB6	0.86 (0.14; 1.80)	18	1.09 (0.34; 1.90)	20	0.762
PSMB7	0.78 (0.10; 2.01)	14	0.91 (0.25; 2.13)	14	0.734
PSMB8	0.81 (0.07; 2.49)	21	1.16 (0.29; 2.75)	27	0.055
PSMB9	0.85 (0.07; 2.17)	22	1.17 (0.49; 3.44)	28	**0.038**
PSMB10	0.91 (0.21; 2.22)	22	1.40 (0.21; 2.98)	29	**0.013**
PSMC3	1.09 (0.13; 1.78)	22	1.29 (0.47; 2.02)	29	**0.046**
PSMD11	0.99 (0.15; 1.46)	22	1.15 (0.59; 2.10)	28	**0.047**
Proteomics					
PSMA1	3591410.62 (3359946.50; 3743800.25)	10	4061904.12 (3345331.25; 4549314.00)	10	**0.005**
PSMA2	2431286.38 (2306954.00; 2834509.25)	10	2839256.50 (2188927.00; 3094963.00)	10	**0.043**
PSMA3	1780854.38 (1664620.50; 2101618.50)	10	1984160.19 (1631098.38; 2175828.75)	10	0.075
PSMA4	2471428.25 (1849629.38; 2848005.50)	10	2508090.12 (2196625.00; 2980470.75)	10	0.579
PSMA5	2605681.50 (2220650.25; 2920024.50)	10	2769701.38 (2344787.50; 2995570.75)	10	0.481
PSMA6	3163709.88 (2779548.00; 3619051.00)	10	3378434.25 (2742440.50; 3825412.75)	10	0.481
PSMA7	1263953.50 (1186403.25; 1477785.50)	10	1417085.31 (1086828.75; 1531569.00)	10	**0.035**
PSMB1	1710980.25 (1598936.12; 1902005.12)	10	1888870.62 (1537245.12; 2039356.00)	10	**0.035**
PSMB2	1201187.19 (1111193.00; 1337028.38)	10	1498489.44 (1068553.62; 1639947.62)	10	**0.003**
PSMB3	1263751.44 (913176.69; 1439135.38)	10	1237441.88 (1026179.31; 1307308.38)	10	0.393
PSMB4	1916522.50 (1843047.88; 2191820.00)	10	2061837.38 (1685694.12; 2217850.50)	10	0.481
PSMB5 (β5)	40459.57 (27483.93; 51487.94)	10	44590.79 (27497.51; 51008.09)	10	0.481
PSMB6 (β1)	220624.09 (194043.89; 265369.56)	10	216015.51 (195490.25; 323835.56)	10	0.739
PSMB7 (β2)	299550.17 (248406.97; 359454.09)	10	317750.77 (256979.09; 383820.16)	10	0.739
PSMB8 (LMP7)	1334672.56 (1181907.75; 1448009.00)	10	1412297.88 (1127323.50; 1486025.25)	10	0.143
PSMB9 (LMP2)	496345.00 (433016.91; 598412.38)	10	537694.19 (401401.25; 689057.31)	10	0.190
PSMB10 (MECL-1)	1754811.12 (1461945.88; 2323670.50)	10	1693180.38 (1486227.88; 2035762.25)	10	1.000
PSMC1	489425.11 (348500.16; 602909.44)	10	432144.31 (321194.97; 597821.00)	10	0.143
PSMC2	854545.31 (774513.31; 944695.88)	10	796531.47 (714151.38; 857018.81)	10	**0.035**
PSMC3	1735616.31 (1584887.25; 1898117.62)	10	1835529.19 (1694077.25; 2005736.38)	10	0.075

	Control		COPD		*p*-value[B]
	median (min; max)	N	median (min; max)	N	
PSMC4	920758.94 (640120.62; 1059456.00)	10	848032.00 (732012.75; 1447610.50)	10	0.143
PSMC5	929184.84 (743135.56; 1036756.38)	10	912323.16 (702285.38; 1002490.69)	10	0.436
PSMC6	923672.12 (728248.31; 1000605.56)	10	911921.88 (739414.69; 968817.06)	10	0.796
PSMD1	1265624.12 (1173353.00; 1295278.00)	10	1321490.44 (1147965.88; 1468379.75)	10	0.165
PSMD2	1802584.06 (1684570.38; 1962934.25)	10	1900500.19 (1685813.62; 2105961.75)	10	0.247
PSMD3	1093337.31 (1010653.19; 1193038.62)	10	1202214.88 (1050113.12; 1365926.62)	10	**0.023**
PSMD4	265636.88 (218377.58; 414893.62)	10	262776.93 (199935.33; 372890.38)	10	0.684
PSMD5	1967300.19 (623123.25; 2600843.25)	10	1649585.12 (496410.31; 3708020.25)	10	0.796
PSMD6	557833.62 (505110.34; 617109.56)	10	643803.16 (511668.31; 693776.25)	10	0.063
PSMD7	437576.36 (376705.78; 465922.12)	10	477690.92 (391019.47; 529325.00)	10	**0.029**
PSMD8	1101720.75 (677126.19; 1477442.50)	10	1310467.19 (894225.56; 1659051.38)	10	0.165
PSMD9	362829.47 (201751.20; 453434.09)	10	364784.59 (258978.81; 495259.06)	10	0.739
PSMD10	568340.41 (481887.56; 633647.88)	10	581961.50 (495186.38; 727128.06)	10	0.684
PSMD11	799264.81 (747988.06; 880560.75)	10	879384.47 (733057.81; 944852.75)	10	**0.035**
PSMD12	650496.84 (609229.62; 913639.12)	10	795726.34 (589332.62; 887492.06)	10	**0.029**
PSMD13	1005064.66 (921122.44; 1174509.00)	10	1170107.94 (924469.25; 1376921.75)	10	**0.005**
PSMD14	273913.03 (228306.52; 318338.69)	10	252154.52 (192615.58; 287774.75)	10	**0.043**

[A] total cell count, i.e. sum of granulocyte, lymphocyte and monocyte

[B] differences between groups were tested using Wilcoxon rank sum test

Table S4: Significant parameters in the linear regression models from the COPD cohort (reference category: control group)

Table S4: Significant parameters in the linear regression models from the COPD cohort (reference category: control group).

	Model 1				Model 2				Model 3				Model 4				Model 5				Model 6			
	stand. β	**95% CI**	***p*-value**	**n**	**stand. β**	**95% CI**	***p*-value**	**n**	**stand. β**	**95% CI**	***p*-value**	**n**	**stand. β**	**95% CI**	***p*-value**	**n**	**stand. β**	**95% CI**	***p*-value**	**n**	**stand. β**	**95% CI**	***p*-value**	**n**
ABP[A]																								
β1	0.817	(0.233; 1.402)	**0.009**	39	1.078	(0.480; 1.676)	**0.001**	38	0.829	(0.241; 1.416)	**0.010**	38	0.807	(0.204; 1.410)	**0.013**	38	0.992	(0.307; 1.678)	**0.008**	38	1.436	(0.744; 2.129)	**<0.001**	37
qPCR[A]																								
PSMB8	0.582	(0.031; 1.134)	**0.044**	48	0.447	(-0.213; 1.108)	0.192	44	0.234	(-0.464; 0.932)	0.516	44	0.185	(-0.508; 0.878)	0.604	44	0.190	(-0.572; 0.952)	0.628	44	0.114	(-0.716; 0.944)	0.789	42
PSMB9	0.595	(0.057; 1.134)	**0.035**	50	0.513	(-0.119; 1.145)	0.119	46	0.227	(-0.445; 0.899)	0.512	46	0.173	(-0.495; 0.841)	0.614	46	0.136	(-0.587; 0.859)	0.714	46	0.156	(-0.607; 0.919)	0.690	44
PSMB10	0.694	(0.169; 1.219)	**0.013**	51	0.591	(-0.015; 1.197)	0.063	47	0.573	(-0.083; 1.229)	0.095	47	0.511	(-0.149; 1.170)	0.137	47	0.503	(-0.202; 1.209)	0.170	47	0.401	(-0.354; 1.156)	0.305	45
PSMD11	0.660	(0.128; 1.192)	**0.019**	50	0.713	(0.094; 1.332)	**0.029**	46	0.579	(-0.092; 1.251)	0.099	46	0.533	(-0.141; 1.207)	0.129	46	0.696	(-0.044; 1.436)	0.073	46	0.573	(-0.219; 1.365)	0.165	45
Native Gel[A]																								
20S activity	1.168	(0.544; 1.793)	**0.001**	27	1.423	(0.546; 2.300)	**0.005**	26	1.542	(0.783; 2.302)	**0.001**	26	1.553	(0.770; 2.335)	**0.001**	26	1.658	(0.685; 2.632)	**0.003**	26	1.761	(0.836; 2.687)	**0.002**	24
26S activity	0.563	(-0.179; 1.305)	0.150	27	1.197	(0.249; 2.146)	**0.022**	26	1.208	(0.179; 2.237)	**0.033**	26	1.219	(0.191; 2.247)	**0.031**	26	1.139	(-0.000; 2.278)	0.065	26	1.056	(-0.148; 2.260)	0.105	24

Table S4: Significant parameters in the linear regression models from the COPD cohort (reference category: control group)

	Model 1				Model 2				Model 3				Model 4				Model 5				Model 6			
	stand. β	**95% CI**	***p*-value**	**n**	**stand. β**	**95% CI**	***p*-value**	**n**	**stand. β**	**95% CI**	***p*-value**	**n**	**stand. β**	**95% CI**	***p*-value**	**n**	**stand. β**	**95% CI**	***p*-value**	**n**	**stand. β**	**95% CI**	***p*-value**	**n**
Total activity	0.768	(0.055; 1.481)	**0.045**	27	1.353	(0.426; 2.281)	**0.009**	26	1.393	(0.403; 2.384)	**0.013**	26	1.405	(0.408; 2.403)	**0.012**	26	1.367	(0.259; 2.475)	**0.026**	26	1.327	(0.197; 2.456)	**0.035**	24
20S abundance	1.153	(0.525; 1.782)	**0.001**	27	1.168	(0.329; 2.007)	**0.013**	26	1.392	(0.607; 2.176)	**0.003**	26	1.397	(0.610; 2.183)	**0.003**	26	1.313	(0.442; 2.183)	**0.008**	26	1.534	(0.569; 2.499)	**0.007**	24
26S abundance	0.969	(0.294; 1.643)	**0.009**	27	1.284	(0.351; 2.217)	**0.013**	26	1.216	(0.374; 2.058)	**0.011**	26	1.222	(0.374; 2.070)	**0.011**	26	1.293	(0.171; 2.415)	**0.036**	26	0.889	(-0.338; 2.115)	0.175	24
Total abundance	1.025	(0.363; 1.687)	**0.006**	27	1.335	(0.423; 2.247)	**0.009**	26	1.283	(0.467; 2.099)	**0.006**	26	1.289	(0.466; 2.112)	**0.006**	26	1.353	(0.259; 2.448)	**0.026**	26	0.972	(-0.219; 2.163)	0.129	24
spec. 26S activity	-1.066	(-1.718; -0.414)	**0.004**	27	-0.919	(-1.825; -0.014)	0.060	26	-0.858	(-1.743; 0.026)	0.072	26	-0.858	(-1.730; 0.014)	0.069	26	-1.040	(-2.125; 0.044)	0.076	26	-0.653	(-1.910; 0.605)	0.324	24
spec. Total activity	-1.088	(-1.734; -0.442)	**0.003**	27	-0.982	(-1.890; -0.074)	**0.046**	26	-0.939	(-1.822; -0.056)	0.051	26	-0.938	(-1.806; -0.070)	**0.048**	26	-1.050	(-2.141; 0.041)	0.075	26	-0.574	(-1.801; 0.653)	0.373	24
Proteomics[A]																								
PSMA1	1.258	(0.570; 1.946)	**0.002**	20	1.177	(0.508; 1.847)	**0.004**	20	1.265	(0.474; 2.056)	**0.008**	20	1.231	(0.412; 2.050)	**0.011**	20	1.375	(0.640; 2.109)	**0.003**	20	1.358	(0.564; 2.153)	**0.006**	20
PSMA2	0.933	(0.142; 1.724)	**0.033**	20	0.894	(0.118; 1.669)	**0.039**	20	1.038	(0.090; 1.985)	0.051	20	0.979	(0.003; 1.955)	0.071	20	1.035	(0.080; 1.990)	0.054	20	1.088	(0.061; 2.116)	0.060	20
PSMA7	0.867	(0.061; 1.674)	**0.049**	20	0.730	(-0.013; 1.474)	0.073	20	0.760	(-0.168; 1.688)	0.133	20	0.712	(-0.229; 1.653)	0.162	20	0.643	(-0.282; 1.568)	0.196	20	0.571	(-0.419; 1.561)	0.280	20

Table S4: Significant parameters in the linear regression models from the COPD cohort (reference category: control group)

	Model 1				Model 2				Model 3				Model 4				Model 5				Model 6			
	stand. β	**95% CI**	***p*-value**	**n**	**stand. β**	**95% CI**	***p*-value**	**n**	**stand. β**	**95% CI**	***p*-value**	**n**	**stand. β**	**95% CI**	***p*-value**	**n**	**stand. β**	**95% CI**	***p*-value**	**n**	**stand. β**	**95% CI**	***p*-value**	**n**
PSMB1	0.888	(0.086; 1.690)	**0.044**	20	0.728	(0.036; 1.420)	0.057	20	0.904	(0.082; 1.726)	0.051	20	0.863	(0.008; 1.717)	0.069	20	0.574	(-0.270; 1.417)	0.206	20	0.456	(-0.424; 1.335)	0.330	20
PSMB2	1.324	(0.664; 1.985)	**0.001**	20	1.251	(0.583; 1.919)	**0.002**	20	1.699	(1.018; 2.381)	**<0.001**	20	1.706	(1.008; 2.404)	**<0.001**	20	1.522	(0.774; 2.270)	**0.002**	20	1.343	(0.623; 2.062)	**0.003**	20
PSMC2	-0.946	(-1.733; -0.158)	**0.030**	20	-0.917	(-1.734; -0.101)	**0.044**	20	-0.526	(-1.429; 0.378)	0.275	20	-0.478	(-1.381; 0.424)	0.318	20	-0.519	(-1.430; 0.393)	0.285	20	-0.614	(-1.581; 0.352)	0.237	20
PSMC3	0.926	(0.134; 1.719)	**0.034**	20	0.936	(0.131; 1.741)	**0.038**	20	1.078	(0.174; 1.982)	**0.036**	20	1.091	(0.168; 2.014)	**0.038**	20	0.918	(-0.061; 1.897)	0.089	20	0.948	(-0.110; 2.005)	0.104	20
PSMD1	0.791	(-0.032; 1.614)	0.076	20	0.896	(0.083; 1.708)	**0.047**	20	1.103	(0.131; 2.075)	**0.045**	20	1.084	(0.085; 2.083)	0.053	20	0.960	(-0.058; 1.977)	0.087	20	0.745	(-0.263; 1.752)	0.173	20
PSMD3	1.079	(0.329; 1.829)	**0.011**	20	1.049	(0.251; 1.847)	**0.021**	20	1.183	(0.310; 2.056)	**0.020**	20	1.158	(0.243; 2.073)	**0.028**	20	0.975	(0.008; 1.942)	0.070	20	0.869	(-0.154; 1.892)	0.122	20
PSMD6	0.900	(0.102; 1.699)	**0.040**	20	0.796	(-0.017; 1.609)	0.074	20	0.880	(-0.112; 1.872)	0.106	20	0.839	(-0.161; 1.839)	0.124	20	0.532	(-0.295; 1.360)	0.230	20	0.324	(-0.461; 1.109)	0.435	20
PSMD7	0.999	(0.226; 1.772)	**0.021**	20	1.002	(0.167; 1.836)	**0.033**	20	1.137	(0.172; 2.102)	**0.038**	20	1.122	(0.127; 2.117)	**0.046**	20	1.088	(0.091; 2.085)	0.052	20	1.004	(-0.060; 2.069)	0.089	20
PSMD11	0.960	(0.176; 1.743)	**0.027**	20	0.960	(0.135; 1.785)	**0.038**	20	0.950	(0.127; 1.772)	**0.041**	20	0.942	(0.087; 1.798)	0.050	20	0.817	(-0.084; 1.719)	0.099	20	0.748	(-0.217; 1.712)	0.155	20

Table S4: Significant parameters in the linear regression models from the COPD cohort (reference category: control group)

	Model 1				**Model 2**				**Model 3**				**Model 4**				**Model 5**				**Model 6**			
	stand. β	**95% CI**	***p*-value**	**n**	**stand. β**	**95% CI**	***p*-value**	**n**	**stand. β**	**95% CI**	***p*-value**	**n**	**stand. β**	**95% CI**	***p*-value**	**n**	**stand. β**	**95% CI**	***p*-value**	**n**	**stand. β**	**95% CI**	***p*-value**	**n**
PSMD12	1.032	(0.268; 1.796)	**0.016**	20	0.986	(0.191; 1.780)	**0.028**	20	0.855	(-0.120; 1.831)	0.109	20	0.804	(-0.173; 1.781)	0.131	20	0.664	(-0.227; 1.556)	0.168	20	0.651	(-0.313; 1.616)	0.210	20
PSMD13	1.281	(0.603; 1.960)	**0.002**	20	1.204	(0.499; 1.909)	**0.004**	20	1.271	(0.397; 2.145)	**0.014**	20	1.220	(0.328; 2.112)	**0.019**	20	1.135	(0.254; 2.016)	**0.025**	20	1.093	(0.143; 2.042)	**0.044**	20
PSMD14	-0.971	(-1.752; -0.191)	**0.025**	20	-0.903	(-1.725; -0.080)	**0.048**	20	-0.824	(-1.757; 0.108)	0.107	20	-0.776	(-1.706; 0.155)	0.126	20	-0.900	(-1.874; 0.074)	0.093	20	-1.017	(-2.042; 0.009)	0.076	20

[A]scaled to have mean=0 and SD=1

Model 1: crude model (i.e. unadjusted)

Model 2: adjusted for sex, age and BMI

Model 3: adjusted for sex, age, BMI, comorbidities and percentage granulocytes

Model 4: adjusted for sex, age, BMI, comorbidities and percentage lymphocytes

Model 5: adjusted for sex, age, BMI, comorbidities and leukocytes (in µl, i.e. total cell count defined as sum of granulocytes, lmyphocytes and monocytes)

Model 6: adjusted for sex, age, BMI, comorbidities, leukocytes (in µl, i.e. total cell count defined as sum of granulocytes, lymphocytes and monocytes) and immunosuppressive medication

Table S5: Sensitivity Analysis: **Same parameters in the linear regression models without ever-smoking controls (reference category: control group)**

Table S5: Sensitivity Analysis: Same parameters in the linear regression models without ever-smoking controls (reference category: control group).

	Model 1				Model 2				Model 3				Model 4				Model 5				Model 6			
	stand. β	**95% CI**	***p*-value**	**n**	**stand. β**	**95% CI**	***p*-value**	**n**	**stand. β**	**95% CI**	***p*-value**	**n**	**stand. β**	**95% CI**	***p*-value**	**n**	**stand. β**	**95% CI**	***p*-value**	**n**	**stand. β**	**95% CI**	***p*-value**	**n**
ABP[A]																								
β1	0.699	(-0.001; 1.398)	0.060	32	0.940	(0.249; 1.631)	**0.013**	31	0.722	(0.050; 1.394)	**0.046**	31	0.710	(0.021; 1.399)	0.055	31	0.868	(0.048; 1.687)	**0.049**	31	1.267	(0.471; 2.063)	**0.005**	30
qPCR[A]																								
PSMB8	0.380	(-0.267; 1.027)	0.257	41	0.242	(-0.508; 0.993)	0.532	37	0.010	(-0.785; 0.806)	0.980	37	-0.035	(-0.822; 0.752)	0.931	37	-0.246	(-1.092; 0.599)	0.572	37	-0.270	(-1.188; 0.648)	0.570	35
PSMB9	0.493	(-0.132; 1.119)	0.130	43	0.394	(-0.319; 1.107)	0.286	39	0.088	(-0.662; 0.838)	0.820	39	0.034	(-0.707; 0.776)	0.928	39	-0.172	(-0.943; 0.599)	0.665	39	-0.137	(-0.944; 0.670)	0.741	37
PSMB10	0.597	(-0.021; 1.215)	0.065	44	0.501	(-0.187; 1.189)	0.163	40	0.465	(-0.255; 1.185)	0.214	40	0.395	(-0.325; 1.116)	0.290	40	0.247	(-0.518; 1.013)	0.531	40	0.161	(-0.651; 0.973)	0.700	38
PSMD11	0.546	(-0.044; 1.135)	0.077	43	0.605	(-0.054; 1.265)	0.081	39	0.407	(-0.280; 1.095)	0.254	39	0.357	(-0.328; 1.042)	0.314	39	0.462	(-0.312; 1.236)	0.250	39	0.337	(-0.481; 1.155)	0.426	38
Native Gel[A]																								
20S activity	1.200	(0.442; 1.958)	**0.006**	22	1.589	(0.553; 2.624)	**0.008**	21	1.654	(0.810; 2.498)	**0.002**	21	1.652	(0.769; 2.535)	**0.003**	21	2.189	(0.648; 3.730)	**0.015**	21	1.975	(0.480; 3.470)	**0.025**	19
26S activity	0.567	(-0.340; 1.473)	0.235	22	1.215	(0.063; 2.368)	0.055	21	1.229	(-0.010; 2.468)	0.072	21	1.235	(-0.004; 2.475)	0.071	21	0.589	(-1.265; 2.443)	0.543	21	0.323	(-1.567; 2.213)	0.744	19

Table S5: Sensitivity Analysis: **Same parameters in the linear regression models without ever-smoking controls (reference category: control group)**

	Model 1				Model 2				Model 3				Model 4				Model 5				Model 6			
	stand. β	**95% CI**	***p*-value**	**n**	**stand. β**	**95% CI**	***p*-value**	**n**	**stand. β**	**95% CI**	***p*-value**	**n**	**stand. β**	**95% CI**	***p*-value**	**n**	**stand. β**	**95% CI**	***p*-value**	**n**	**stand. β**	**95% CI**	***p*-value**	**n**
Total activity	0.779	(-0.094; 1.653)	0.096	22	1.412	(0.288; 2.535)	**0.026**	21	1.440	(0.258; 2.621)	**0.032**	21	1.445	(0.250; 2.639)	**0.033**	21	1.058	(-0.764; 2.880)	0.274	21	0.784	(-1.021; 2.589)	0.413	19
20S abundance	1.195	(0.453; 1.936)	**0.005**	22	1.320	(0.360; 2.279)	**0.016**	21	1.451	(0.595; 2.307)	**0.005**	21	1.450	(0.594; 2.307)	**0.005**	21	1.760	(0.458; 3.061)	**0.019**	21	1.787	(0.299; 3.276)	**0.038**	19
26S abundance	0.978	(0.145; 1.810)	**0.032**	22	1.321	(0.179; 2.464)	**0.038**	21	1.284	(0.295; 2.273)	**0.023**	21	1.278	(0.269; 2.287)	**0.026**	21	1.420	(-0.470; 3.311)	0.163	21	0.861	(-1.197; 2.918)	0.430	19
Total abundance	1.037	(0.220; 1.854)	**0.022**	22	1.381	(0.265; 2.497)	**0.027**	21	1.354	(0.394; 2.313)	**0.015**	21	1.348	(0.368; 2.327)	**0.017**	21	1.508	(-0.336; 3.351)	0.131	21	0.961	(-1.036; 2.959)	0.366	19
spec. 26S activity	-1.186	(-1.962; -0.410)	**0.007**	22	-1.094	(-2.154; -0.034)	0.060	21	-1.013	(-1.963; -0.062)	0.055	21	-1.006	(-1.961; -0.052)	0.058	21	-2.157	(-3.712; -0.602)	**0.017**	21	-1.854	(-3.642; -0.065)	0.067	19
spec. Total activity	-1.182	(-1.953; -0.411)	**0.007**	22	-1.091	(-2.167; -0.015)	0.064	21	-1.032	(-2.046; -0.018)	0.066	21	-1.025	(-2.029; -0.020)	0.065	21	-1.959	(-3.624; -0.294)	0.037	21	-1.548	(-3.375; 0.279)	0.125	19
Proteomics[A]																								
PSMA1	1.170	(0.414; 1.927)	**0.008**	18	1.140	(0.395; 1.885)	**0.010**	18	1.285	(0.400; 2.170)	**0.016**	18	1.258	(0.346; 2.170)	**0.021**	18	1.454	(0.692; 2.217)	**0.003**	18	1.381	(0.582; 2.179)	**0.007**	18
PSMA2	0.818	(-0.054; 1.691)	0.085	18	0.811	(-0.057; 1.679)	0.090	18	1.002	(-0.055; 2.058)	0.090	18	0.953	(-0.132; 2.038)	0.113	18	1.058	(0.018; 2.099)	0.072	18	1.059	(-0.063; 2.182)	0.094	18
PSMA7	0.702	(-0.172; 1.576)	0.135	18	0.625	(-0.200; 1.451)	0.162	18	0.684	(-0.347; 1.715)	0.220	18	0.647	(-0.397; 1.690)	0.250	18	0.602	(-0.432; 1.636)	0.278	18	0.513	(-0.577; 1.603)	0.378	18

Table S5: Sensitivity Analysis: **Same parameters in the linear regression models without ever-smoking controls (reference category: control group)**

	Model 1				Model 2				Model 3				Model 4				Model 5				Model 6			
	stand. β	**95% CI**	***p*-value**	**n**	**stand. β**	**95% CI**	***p*-value**	**n**	**stand. β**	**95% CI**	***p*-value**	**n**	**stand. β**	**95% CI**	***p*-value**	**n**	**stand. β**	**95% CI**	***p*-value**	**n**	**stand. β**	**95% CI**	***p*-value**	**n**
PSMB1	0.712	(-0.149; 1.574)	0.125	18	0.625	(-0.131; 1.382)	0.129	18	0.877	(-0.010; 1.763)	0.079	18	0.852	(-0.064; 1.768)	0.095	18	0.590	(-0.347; 1.526)	0.243	18	0.443	(-0.489; 1.376)	0.373	18
PSMB2	1.323	(0.593; 2.054)	**0.003**	18	1.295	(0.549; 2.041)	**0.005**	18	1.732	(0.960; 2.504)	**0.001**	18	1.738	(0.950; 2.525)	**0.001**	18	1.550	(0.702; 2.399)	**0.004**	18	1.374	(0.588; 2.160)	**0.006**	18
PSMC2	-0.670	(-1.431; 0.090)	0.103	18	-0.687	(-1.511; 0.137)	0.126	18	-0.389	(-1.287; 0.509)	0.414	18	-0.373	(-1.289; 0.542)	0.441	18	-0.473	(-1.445; 0.498)	0.360	18	-0.518	(-1.559; 0.522)	0.352	18
PSMC3	0.878	(0.016; 1.739)	0.063	18	0.816	(-0.037; 1.670)	0.084	18	1.077	(0.121; 2.034)	**0.049**	18	1.112	(0.153; 2.070)	**0.044**	18	1.004	(-0.011; 2.019)	0.079	18	0.955	(-0.132; 2.042)	0.116	18
PSMD1	0.870	(-0.048; 1.787)	0.082	18	0.912	(-0.010; 1.834)	0.075	18	1.139	(0.036; 2.242)	0.068	18	1.119	(-0.011; 2.249)	0.078	18	0.997	(-0.157; 2.152)	0.118	18	0.781	(-0.323; 1.885)	0.196	18
PSMD3	1.082	(0.259; 1.906)	**0.020**	18	1.052	(0.177; 1.927)	**0.035**	18	1.269	(0.305; 2.233)	**0.026**	18	1.249	(0.243; 2.254)	**0.033**	18	1.084	(0.013; 2.155)	0.073	18	0.949	(-0.149; 2.046)	0.121	18
PSMD6	0.854	(-0.041; 1.750)	0.080	18	0.769	(-0.150; 1.687)	0.125	18	0.912	(-0.187; 2.012)	0.132	18	0.885	(-0.224; 1.994)	0.146	18	0.572	(-0.365; 1.509)	0.256	18	0.373	(-0.487; 1.234)	0.415	18
PSMD7	0.999	(0.132; 1.867)	**0.038**	18	1.004	(0.059; 1.948)	0.058	18	1.163	(0.066; 2.260)	0.062	18	1.146	(0.018; 2.273)	0.072	18	1.126	(0.000; 2.252)	0.076	18	1.024	(-0.160; 2.208)	0.121	18
PSMD11	0.964	(0.131; 1.796)	**0.038**	18	0.983	(0.102; 1.863)	**0.048**	18	1.063	(0.162; 1.964)	**0.041**	18	1.057	(0.124; 1.991)	**0.048**	18	0.948	(-0.039; 1.935)	0.086	18	0.848	(-0.183; 1.879)	0.138	18

Table S5: Sensitivity Analysis: **Same parameters in the linear regression models without ever-smoking controls (reference category: control group)**

	Model 1				Model 2				Model 3				Model 4				Model 5				Model 6			
	stand. β	**95% CI**	***p*-value**	**n**	**stand. β**	**95% CI**	***p*-value**	**n**	**stand. β**	**95% CI**	***p*-value**	**n**	**stand. β**	**95% CI**	***p*-value**	**n**	**stand. β**	**95% CI**	***p*-value**	**n**	**stand. β**	**95% CI**	***p*-value**	**n**
PSMD12	0.909	(0.070; 1.747)	0.050	18	0.891	(0.005; 1.776)	0.070	18	0.802	(-0.286; 1.890)	0.176	18	0.764	(-0.326; 1.855)	0.197	18	0.630	(-0.381; 1.641)	0.247	18	0.617	(-0.473; 1.706)	0.293	18
PSMD13	1.277	(0.520; 2.033)	**0.004**	18	1.227	(0.442; 2.012)	**0.009**	18	1.354	(0.385; 2.323)	**0.019**	18	1.308	(0.320; 2.296)	**0.025**	18	1.232	(0.250; 2.215)	**0.032**	18	1.173	(0.125; 2.221)	0.053	18
PSMD14	-0.876	(-1.731; -0.022)	0.062	18	-0.849	(-1.768; 0.070)	0.094	18	-0.738	(-1.784; 0.309)	0.194	18	-0.693	(-1.736; 0.349)	0.219	18	-0.821	(-1.917; 0.275)	0.170	18	-0.943	(-2.080; 0.194)	0.135	18

[A]scaled to have mean=0 and SD=1

Model 1: crude model (i.e. unadjusted)

Model 2: adjusted for sex, age and BMI

Model 3: adjusted for sex, age, BMI, comorbidities and percentage granulocytes

Model 4: adjusted for sex, age, BMI, comorbidities and percentage lymphocytes

Model 5: adjusted for sex, age, BMI, comorbidities and leukocytes (in µl, i.e. total cell count defined as sum of granulocytes, lmyphocytes and monocytes)

Model 6: adjusted for sex, age, BMI, comorbidities, leukocytes (in µl, i.e. total cell count defined as sum of granulocytes, lymphocytes and monocytes) and immunosuppressive medication

SUPPLEMENTARY REFERENCES

1. Keller IE, Vosyka O, Takenaka S, Kloß A, Dahlmann B, Willems LI, Verdoes M, Overkleeft HS, Marcos E, Adnot S, Hauck SM, Ruppert C, Günther A, Herold S, Ohno S, Adler H, Eickelberg O, Meiners S. Regulation of Immunoproteasome Function in the Lung. *Scientific Reports* 2015; 5: 10230.

2. Wiśniewski JR, Zougman A, Nagaraj N, Mann M. Universal sample preparation method for proteome analysis. *Nature methods* 2009; 6: 359–362.

3. Grosche A, Hauser A, Lepper MF, Mayo R, von Toerne C, Merl-Pham J, Hauck SM. The Proteome of Native Adult Müller Glial Cells From Murine Retina. *Molecular & cellular proteomics : MCP* 2016; 15: 462–480.

4. Lepper MF, Ohmayer U, von Toerne C, Maison N, Ziegler A-G, Hauck SM. Proteomic Landscape of Patient-Derived CD4+ T Cells in Recent-Onset Type 1 Diabetes. *Journal of Proteome Research* 2018; 17: 618–634.

5. Mattugini N, Merl-Pham J, Petrozziello E, Schindler L, Bernhagen J, Hauck SM, Götz M. Influence of white matter injury on gray matter reactive gliosis upon stab wound in the adult murine cerebral cortex. *Glia* 2018; 66: 1644–1662.

6. Bruderer R, Bernhardt OM, Gandhi T, Miladinović SM, Cheng L-Y, Messner S, Ehrenberger T, Zanotelli V, Butscheid Y, Escher C, Vitek O, Rinner O, Reiter L. Extending the Limits of Quantitative Proteome Profiling with Data-Independent Acquisition and Application to Acetaminophen-Treated Three-Dimensional Liver Microtissues. *Molecular & Cellular Proteomics* 2015; 14: 1400–1410.

7. Metsalu T, Vilo J. ClustVis: a web tool for visualizing clustering of multivariate data using Principal Component Analysis and heatmap. *Nucleic Acids Res* 2015; 43: W566–W570.

8. Quanjer PH, Stanojevic S, Cole TJ, Baur X, Hall GL, Culver BH, Enright PL, Hankinson JL, Ip MSM, Zheng J, Stocks J, ERS Global Lung Function Initiative. Multi-ethnic reference values for spirometry for the 3-95-yr age range: the global lung function 2012 equations. *Eur Respir J* 2012; 40: 1324–1343.

9. Rieckmann JC, Geiger R, Hornburg D, Wolf T, Kveler K, Jarrossay D, Sallusto F, Shen-Orr SS, Lanzavecchia A, Mann M, Meissner F. Social network architecture of human immune cells unveiled by quantitative proteomics. *Nature Immunology* 2017; 18: 583–593.